Table of Contents

SYLLABUS

Course Catalog

3 Credit hours (3 h lectures). Components, advantages and classifications of fiber communication systems. Dielectric slab waveguide. Step index fiber. Graded index fiber. Attenuation and dispersion. Light sources. Optical modulation. Photodetectors. Optical detection. Noise in the optical receiver. Heterodyne detection. Bit error rate analysis of direct detection and heterodyne detection systems.

Textbook

Optical Fiber Communications, G. Keiser, McGraw Hill, 4^{th} edition.

References

1- Fiber-optic Communication Systems, G. Agrawal, 2^{nd} edition, Wiley,1997.

2- Optical Fiber Communications, J. Senior, Prentice Hall, 2^{nd} edition, 1992.

Instructor

Instructor: Dr. Mohammad M. Banat

Email Address: banat@just.edu.jo

Prerequisites

By topics: Electromagnetics, Digital communications.

By course numbers: EE 307, EE 551.

Prerequisite for: none.

Topics Covered

Week	Topics	Chepters in Text
1	Overview of optical fiber communications.	
2-3	Optical fibers: structures, types, propagating modes, materials, and fabrication methods.	
4-5	Optical fibers: attenuation, dispersion, dispersion compensation fibers, and fiber-fiber coupling.	
6-7	Optical sources: semiconductor lasers, light emitting diodes, and power launching & coupling.	
8-9	photodetectors: p-i-n photodiodes, avalanche photodiodes, and shot noise.	
10-11	Optical receivers: photodetectors, preamplifiers, filters, and noise sources.	
12-15	Optical fiber communication system: design and performance of digital links.	

Objectives and Outcomes

Objectives	Outcomes
1. Studying the components, advantages, and the role of optical fiber communication systems in communication networks [1,2]	1.1. Knowing the advantages, and the role of optical fiber communication systems in communication networks [1,2]
2. Studying the structures, types, propagating modes, materials, and fabrication methods of optical fibers [1,2]	2.1. Understanding the structures, types, propagating modes, materials, and fabrication methods of optical fibers [1,2]
3. Studying the attenuation and dispersion mechanisms in optical fibers and the design of dispersion compensation fibers [1,2]	3.1. Understanding the attenuation and dispersion mechanisms in optical fibers and the design of dispersion compensation fibers [1,2]
4. Studying the different types of optical sources (semiconductor lasers and light emitting diodes) and power launching & coupling methods [1,2]	4.1. Knowing the different types of optical sources used in optical fiber communication system and also the power launching & coupling methods [1,2]
5. Studying the different types of photodetectors (p-i-n photodiodes and avalanche photodiodes), and the noise sources in optical receivers [1,2]	5.1. Knowing the different types of photodetectors used in optical fiber communication systems and also the noise sources in optical receivers [1,2]
6. Learning the design of a digital link using optical fiber communication system [1,2]	6.1. Ability to design a digital link using optical fiber communication systems [1,2]

Evaluation

Assessment Tool	Expected Due Date	Weight
Mid-Term Exam		25%
Term Project Report		10%
Term Project Presentation		15%
Final Exam		50%

Contribution of Course to Meeting the Professional Component

The course contributes to building the fundamental basic concepts, applications, and design of Electrical Engineering.

Relationship to Program Outcomes (%)

1	2	3	4	5	6	7
50	50					

I. INTRODUCTION

Lightwave systems represent a natural extension of microwave communication systems in the sense that information is transmitted over an electromagnetic carrier in both types of systems. The major difference is that, whereas carrier frequency is typically around 1 GHz for microwave systems, it increases by five orders of magnitude, and is typically around 100 THz in the case of lightwave systems. This increase in carrier frequency translates into a corresponding increase in the system capacity. Whereas microwave systems rarely operate above 0.2 Gb/s, commercial lightwave systems can operate at bit rates exceeding 1 Tb/s.

Although the optical carrier is transmitted in free space for some applications related to satellites and space research, terrestrial lightwave systems often employ optical fibers for information transmission. Such fiber-optic communication systems have been deployed worldwide since 1980 and constitute the backbone behind the Internet. One can even claim that the lightwave technology together with advances in microelectronics was responsible for the advent of the "information age" by the end of the twentieth century.

I.1. Evolution of Lightwave Systems

Microwave communication systems were commercialized during the decade of 1940s, and carrier frequencies of up to 4 GHz were used by 1947 for commercial systems. During the following 25 years or so, microwave as well as coaxial systems evolved considerably. Although such systems were able to operate at bit rates of up to 200 Mb/s or so, they were approaching the fundamental limits of the technology behind them. It was realized in the 1950s that an increase of several orders of magnitude in the system capacity should be possible if optical waves were used in place of microwaves as the carrier of information.

Neither a coherent optical source, nor a suitable transmission medium, was available during the 1950s. The invention of the laser somehow solved the first problem. Attention was then focused on finding ways of transmitting laser light over long distances. In contrast with the microwaves, optical beams suffer from many problems when they are transmitted through the atmosphere.

Optical glass fibers were developed during the 1950s, mainly for medical applications. It was suggested in 1966 that optical fibers might be the best choice for transporting optical signals in lightwave systems; as they are capable of guiding the light in a manner similar to the guiding of electrons in copper wires. The main problem was their high losses; since fibers available during the 1960s had losses in excess of 1,000 dB/km.

A breakthrough occurred in 1970 when fiber losses were reduced to below 20 dB/km in the wavelength region near 1 μm using a novel fabrication technique. At about the same time, GaAs semiconductor lasers, operating continuously at room temperature, were demonstrated. The simultaneous availability of compact optical sources and low-loss optical fibers led to a worldwide effort for developing fiber-optic communication systems during the 1970s. Terrestrial lightwave systems became available commercially beginning in 1980.

Figure I.1 shows the increase in the capacity of lightwave systems realized after 1980 through several generations of development. The progress has indeed been rapid as evident from an increase in the system capacity by a factor of 100,000 over a period of less than 25 years. The saturation of the capacity after 2000 is partly due to the economic slowdown experienced by the lightwave industry (known popularly as the bursting of the telecom bubble). The change in the slope after 1992 is due to the advent of WDM technology.

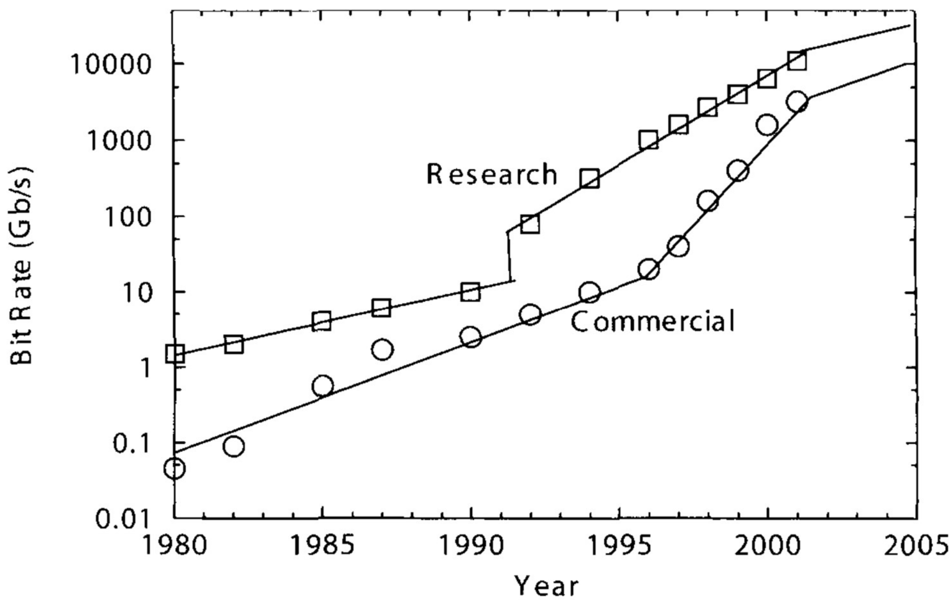

Figure I.1: Increase in the capacity of lightwave systems realized after 1980

The distance over which a lightwave system can transmit data without introducing errors is also important while judging the system performance. Since signals are degraded during transmission, most lightwave systems require periodic regeneration of the optical signal through devices known as "repeaters." A commonly used figure of merit for any communication system is the bit rate-distance product, BL, where B is the bit rate and L is the repeater spacing.

The research phase of lightwave systems started around 1975. The first-generation systems operated in the near infrared[1] at a wavelength close to 800 nm and used GaAs semiconductor lasers as an optical source. They were able to work at a bit rate of 45 Mb/s and allowed repeater spacings of up to 10 km. The 10-km value may seem too small from a modern perspective, but it was 10 times larger than the 1-km spacing prevalent at that time in coaxial systems. The enormous progress realized over the 25-year period extending from 1975 to 2000 can be grouped into four distinct generations. Figure I.2 shows the increase in the BL product over this time period as quantified through various laboratory experiments. The straight line corresponds to a doubling of the BL product every year. In every generation, BL increases initially but then saturates as the

[1] Infrared radiation (IR), also known as thermal radiation, is that band in the electromagnetic radiation spectrum with wavelengths above red visible light between 780 nm and 1 mm. IR is categorized as IR-A (780 nm-1.4 μm), IR-B (1.4-3 μm) and IR-C, also known as far-IR (3 μm-1 mm). Visible light spans the range 400 to 780 nm.

technology matures. Each new generation brings a fundamental change that helps to improve the system performance further.

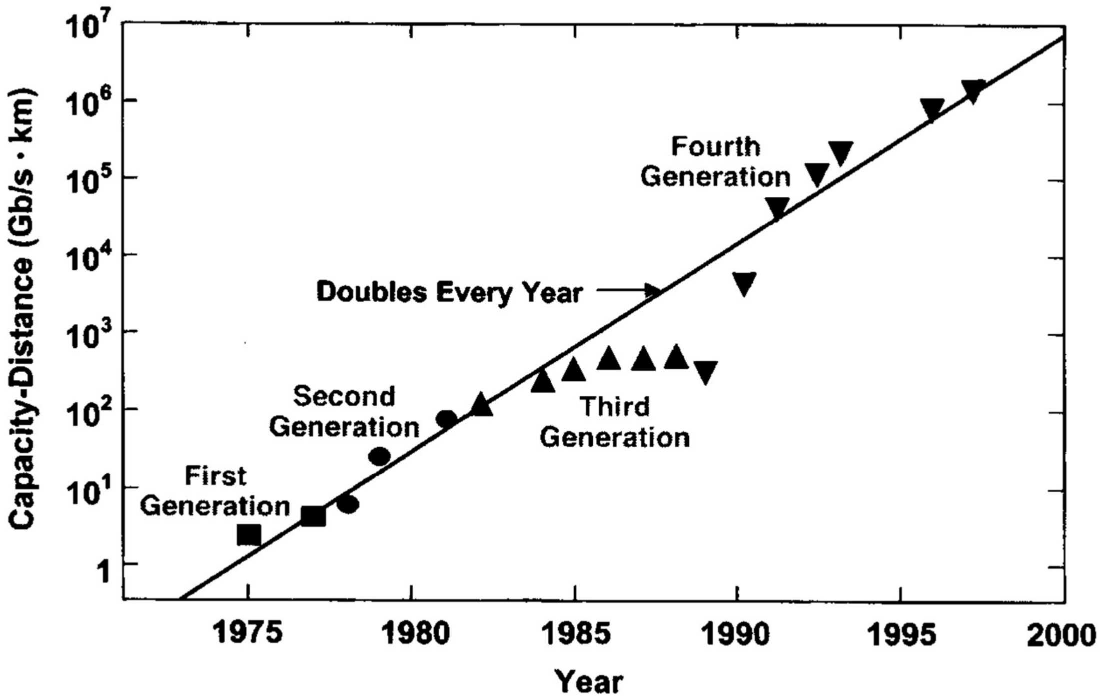

Figure I.2: Increase in the *BL* product from 1975 to 2000

It was clear during the 1970s that the repeater spacing could be increased considerably by operating the lightwave system in the wavelength region near 1.3 μm, where fiber losses were below 0.5 dB/km. Furthermore, optical fibers exhibit minimum dispersion in this wavelength region. This realization led to a worldwide effort for the development of semiconductor lasers and detectors operating near 1.3 μm.

The second generation of fiber-optic communication systems became available in the early 1980s, but the bit rate of early systems was limited to below 100 Mb/s because of dispersion in multimode fibers. This limitation was overcome by the use of single-mode fibers. A laboratory experiment in 1981 demonstrated transmission at 2 Gb/s over 44 km of single-mode fiber. The introduction of commercial systems soon followed. By 1987, second-generation lightwave systems, operating at bit rates of up to 1.7 Gb/s with a repeater spacing of about 50 km, were commercially available.

The repeater spacing of the second-generation lightwave systems was limited by fiber losses at the operating wavelength of 1.3 μm (typically 0.5 dB/km). **Losses of silica fibers become minimum near 1.55 μm.** A 0.2-dB/km loss was realized in 1979 in this spectral region. However, the introduction of third-generation lightwave systems operating at 1.55 μm was considerably delayed by a relatively large dispersion of standard optical fibers in the wavelength region near 1.55 μm. The dispersion problem can be overcome either by using **dispersion-shifted fibers** designed to have minimum dispersion near 1.55 μm or by limiting the laser spectrum to a single longitudinal mode. Both approaches were followed during the 1980s. By 1985, laboratory experiments indicated the possibility of transmitting information at bit rates of up to 4 Gb/s over distances in excess of 100 km. Third-generation lightwave systems operating at 2.5 Gb/s became available commercially in 1990. Such systems are capable of operating at a bit rate of up to 10 Gb/s. The best performance is achieved using dispersion-shifted fibers in combination with distributed-feedback (DFB) semiconductor lasers.

A drawback of third-generation 1.55-μm systems was that the optical signal had to be regenerated periodically using electronic repeaters after 60 to 70 km of transmission because of fiber losses. Repeater spacing could be increased by 10 to 20 km using homodyne or heterodyne detection schemes because their use requires less power at the receiver. Such coherent lightwave systems were studied during the 1980s and their potential benefits were demonstrated in many system experiments. However, commercial introduction of such systems was postponed with the advent of fiber amplifiers in 1989.

The fourth generation of lightwave systems makes use of optical amplification for increasing the repeater spacing and of wavelength-division multiplexing (WDM) for increasing the bit rate. The advent of the WDM technique started a revolution that resulted in doubling of the system capacity every 6 months or so and led to lightwave systems operating at a bit rate of 10 Tb/s by 2001. In most WDM systems, fiber losses are compensated periodically using erbium-doped fiber amplifiers (EDFAs) spaced 60 to 80 km apart. Such amplifiers were developed after 1985 and became available commercially by 1990. A 1991 experiment showed the possibility of data transmission over 21,000 km at 2.5 Gb/s, and over 14,300 km at 5 Gb/s. This performance indicated that an amplifier-based, all-optical, submarine transmission system was feasible for intercontinental communication. By 1996, not only transmission over 11,300 km at a bit rate of 5 Gb/s had been demonstrated by using actual submarine cables, but commercial transatlantic and transpacific cable systems also became available. Since then, a large number of submarine lightwave systems have been deployed worldwide.

The 27,000-km fiber-optic link around the globe (FLAG) became operational in 1998, linking many Asian and European countries. Another major lightwave system, known as Africa One, was operational by 2000; it circles the African continent and covers a total transmission distance of about 35,000 km. Several WDM systems were deployed across the Atlantic and Pacific oceans from 1998 to 2001 in response to the Internet-induced increase in the data traffic; they have increased the total capacity by orders of magnitudes. One can indeed say that the fourth generation of lightwave systems led to an information revolution that was fuelled by the advent of the Internet.

At the dawn of the twenty-first century, the emphasis of lightwave systems was on increasing the system capacity by transmitting more and more channels through the WDM technique. With increasing WDM signal bandwidth, it was often not possible to amplify all channels using a single amplifier. As a result, new kinds of amplification schemes were explored for covering the spectral region extending from 1.45 to 1.62 μm. This approach led in 2000 to a 3.28-Tb/s experiment in which 82 channels, each operating at 40 Gb/s, were transmitted over 3,000 km, resulting in a BL product of almost 10,000 (Tb/s)-km. Within a year, the system capacity could be increased to nearly 11 Tb/s (273 WDM channels, each operating at 40 Gb/s) but the transmission distance was limited to 117 km. By 2003, in a record experiment 373 channels, each operating at 10 Gb/s, were transmitted over 11,000 km, resulting in a BL product of more than 41,000 (Tb/s)-km. On the commercial side, terrestrial systems with the capacity of 1.6 Tb/s were available by the end of 2000. Given that the first generation systems had a bit rate of only 45 Mb/s in 1980, it is remarkable that the capacity of lightwave systems jumped by a factor of more than 30,000 over a period of only 20 years.

The pace slowed down considerably during the economic turndown in the lightwave industry that began in 2000 and was not completely over in 2004. Although commercial deployment of new lightwave systems virtually halted during this period, the research phase has continued worldwide and is moving toward the fifth generation of lightwave systems. This new generation is concerned with extending the wavelength range over which a WDM system can operate simultaneously. The conventional wavelength window, known as the C band, covers the wavelength range of 1.53 to 1.57 µm. It is being extended on both the long- and short-wavelength sides, resulting in the L and S bands, respectively. The traditional EDFAs are unable to work over such a wide spectral region. For this reason, the Raman amplification technique, well known from earlier research performed in the 1980s, has been readopted for lightwave systems as it can work in all three wavelength bands using suitable pump lasers. A new kind of fiber, known as the dry fiber, has been developed with the property that fiber losses are small over the entire wavelength region extending from 1.30 to 1.65 µm. Research has also continued in several other directions to realize optical fibers with suitable loss and dispersion characteristics. Most noteworthy are photonic-crystal fibers whose dispersion can be changed drastically using an array of holes within the cladding layer. Such fibers have the potential of transmitting optical signal with virtually no losses and little nonlinear distortion!

The fifth-generation systems also attempt to enhance the spectral efficiency by adopting new modulation formats, while increasing the bit rate of each WDM channel. Starting in 1996, many experiments used channels operating at 40 Gb/s, and by 2003 such 40-Gb/s lightwave systems had reached the commercial stage. At the same time, the research phase has moved toward WDM systems with 160 Gb/s per channel. Such systems require an extremely careful management of fiber dispersion. Novel techniques capable of compensating chromatic and polarization-mode dispersions in a dynamic fashion have been developed to meet such challenges. An interesting approach is based on the concept of optical solitons-pulses that preserve their shape during propagation in a lossless fiber by counteracting the effect of dispersion through the fiber nonlinearity. Although the basic idea was proposed as early as 1973, it was only in 1988 that a laboratory experiment demonstrated the feasibility of data transmission over 4,000 km by compensating fiber losses through Raman amplification. Since then, many system experiments have demonstrated the eventual potential of soliton communication systems. Starting in 1996, the WDM technique was also used for solitons in combination with dispersion-management and Raman amplification schemes. Many new modulation formats have been proposed for advancing the state of the art.

I.2. Components of a Lightwave System

Figure I.3 shows a generic optical communication system consisting of an optical transmitter, a communication channel, and an optical receiver.

Figure I.3: A generic optical communication system

Lightwave systems can be classified into two broad categories depending on the nature of the communication channel. The optical signal propagates unguided in air or vacuum for some applications. In other applications, the optical beam emitted by the transmitter remains spatially confined inside an optical fiber. This course focuses mainly on such fiber-optic communication systems.

I.2.A. Optical Transmitters

The role of optical transmitters is to convert an electrical signal into an optical form and to launch the resulting optical signal into the optical fiber acting as a communication channel. Figure I.4 shows the block diagram of an optical transmitter. It consists of an optical source, a modulator, and electronic circuits used to power and operate the two devices. Semiconductor lasers or light-emitting diodes are used as optical sources because of their compact nature and compatibility with optical fibers.

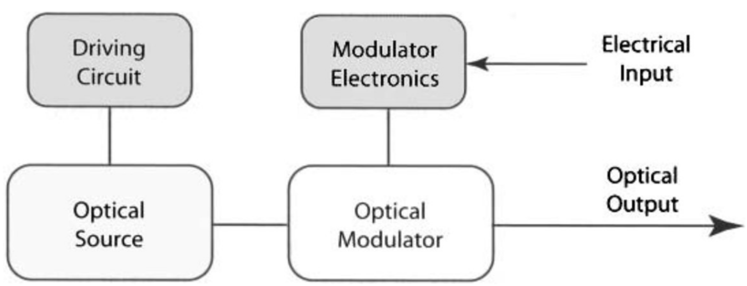

Figure I.4: Block diagram of an optical transmitter

The source emits light in the form of a continuous wave at a fixed wavelength λ_0. The carrier frequency f_0 is related to this wavelength as

$$f_0 = \frac{c}{\lambda_0} \tag{I.1}$$

where c is the speed of light in vacuum.

It is common to divide the spectral region near 1.55 μm into two bands known as the conventional or C band and the long-wavelength or L band. The C band covers carrier frequencies from 191 to 196 THz (in steps of 50 GHz) and spans roughly the wavelength range of 1.53 to 1.57 μm. In contrast, L band occupies the range 1.57 to 1.61 μm and covers carrier frequencies from 186 to 191 THz, again in steps of 50 GHz.

It is important to realize that the source wavelength needs to be set precisely for a given choice of the carrier frequency. For example, a channel operating at 193 THz requires an optical source emitting light at a wavelength of 1.5533288 μm if we use the precise value c = 299,792,458 km/s for the speed of light in vacuum. Changing the wavelength by 3.3 to 1.55 μm changes the frequency to 193.414 THz. The difference is 414 GHz.

Before the source light can be launched into the communication channel, the information that needs to be transmitted should be imposed on it. This step is accomplished by an optical modulator in Figure I.4. The modulator uses the data in the form of an electrical signal to modulate the optical carrier. Although an external modulator is often needed at high bit rates, it can be dispensed with at low bit rates using a technique known as direct modulation.

An important design parameter is the average optical power launched into the communication channel. Clearly, it should be as large as possible to enhance the signal-to-noise ratio (SNR) at the receiver end. However, various nonlinear effects limit how much power can be launched at the transmitter end. The launched power is often expressed in "dBm" units with 1 mW acting as the reference level. The general definition is

$$P_{\mathrm{dBm}} = 10 \log_{10} \frac{P}{1\ \mathrm{mW}} \tag{I.2}$$

Thus, 1 mW is 0 dBm, but 1 μW corresponds to -30 dBm. The launched power is rather low (less than -10 dBm) for light-emitting diodes but semiconductor lasers can launch power levels exceeding 5 dBm.

Although light-emitting diodes are useful for some low-end applications related to local-area networking and computer-data transfer, most lightwave systems employ semiconductor lasers as optical sources.

I.2.B. COMMUNICATION CHANNEL

The role of a communication channel is to transport the optical signal from transmitter to receiver with as little loss in quality as possible. Most terrestrial lightwave systems employ optical fibers as the communication channel because they can transmit light with losses as small as 0.2 dB/km when the carrier frequency lies in the spectral region near 1.5 μm. Even then, optical power reduces to only 1% after 100 km. For long-haul lightwave systems, it is common to employ optical amplifiers or regenerators to compensate for fiber losses and boost the signal power back to its original level. Figure I.5 shows how amplifiers or regenerators can be cascaded to transmit optical signal over distances exceeding hundreds and even thousands of kilometers. Fiber losses play an important role in such systems because they determine the repeater or amplifier spacing.

Ideally, a communication channel should not degrade the quality of the optical signal launched into it. In practice, optical fibers broaden light pulses transmitted through them through modal or chromatic dispersion. When optical pulses spread significantly outside their allocated bit slot, the transmitted signal is degraded so severely that it becomes impossible to recover the original signal with high accuracy. The dispersion problem is most severe for multimode fibers. It is for this reason that most modern lightwave systems employ single-mode fibers. Chromatic dispersion still leads to pulse broadening but its impact can be reduced by controlling the spectral width of the optical source or by employing a dispersion-management technique.

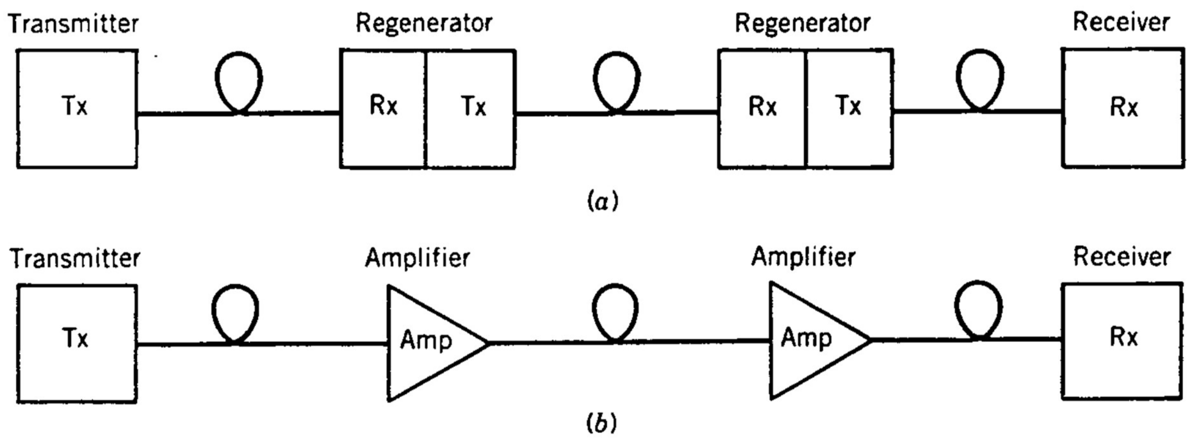

Figure I.5: Optical fiber communication system with regenerators or amplifiers

A third source of signal distortion results from the nonlinear effects related to the intensity dependence of the refractive index of silica. Although most nonlinear effects are relatively weak for silica fibers, they can accumulate to significant levels when many optical amplifiers are cascaded in series to form a long-haul system. Nonlinear effects are especially important for undersea lightwave systems for which the total fiber length can approach thousands of kilometers.

I.2.C. Optical Receivers

An optical receiver converts the optical signal received at the output end of the fiber link back into the original electrical signal. Figure I.6 shows the main components of an optical receiver. Optical signal arriving at the receiver is first directed toward a photodetector that converts it into an electrical form. Semiconductor photodiodes are used as photodetectors because of their compact size and relatively high quantum efficiency. In practice, a p-i-n or an avalanche photodiode produces electric current that varies with time in response to the incident optical signal. It also adds invariably some noise to the signal, thereby reducing the SNR of the electrical signal.

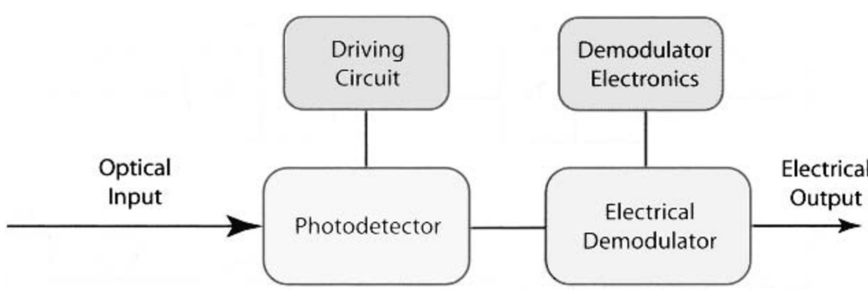

Figure I.6: Optical receiver

The role of the demodulator is to reconstruct the original electrical signal from the time-varying current in spite of the channel-induced degradation and the noise added at the receiver. The design of a demodulator depends on the nature of the signal (analog versus digital) and the modulation format used by the lightwave system. Most modern systems employ a digital binary scheme referred to as **intensify (power) modulation with direct detection**. Demodulation in the digital case is done by a decision circuit that identifies bits as 1 or 0, depending on the amplitude of the electrical signal. The accuracy of the decision circuit depends on the SNR of the electrical signal generated at the photodetector. It is important to design the receiver such that its noise level is not too high.

The performance of a digital lightwave system is characterized through the bit error rate (BER). It is customary to define the BER as the average probability of identifying a bit incorrectly. For example, a BER of 10^{-9} corresponds to on average one error per billion bits. Most lightwave systems specify a BER of less than 10^{-9} as the operating requirement; some even require a BER as small as 10^{-15}. Depending on the system design, it is sometimes not possible to realize such low error rates at the receiver. Error-correcting codes are then used to improve the raw BER of a lightwave system.

An important parameter for any receiver is its sensitivity, defined as the minimum average optical power required to realize a BER of 10^{-9}. Receiver sensitivity depends on the SNR, which in turn depends on various noise sources that corrupt the electrical signal produced at the receiver. Even for a perfect receiver, some noise is introduced by the process of photodetection itself. This quantum noise is referred to as the shot noise as it has its origin in the particle nature of electrons. No practical receiver operates at the quantum-noise limit because of the presence of several other noise sources. Some of the noise sources, such as thermal noise, are internal to the receiver. Others originate at the transmitter or during propagation along the fiber link. For instance, any amplification of the optical signal along the transmission line with the help of optical amplifiers introduces the so-called amplifier noise that has its origin in the fundamental process of spontaneous emission. Several nonlinear effects occurring within optical fibers can manifest as an additional noise that is added to the optical signal during its transmission through the fiber link. The receiver sensitivity is determined by a cumulative effect of all possible noise mechanisms that degrade the SNR at the decision circuit. In general, it also depends on the bit rate as the contribution of some noise sources (e.g., shot noise) increases in proportion to the signal bandwidth.

I.3. Electrical Signals

In any communication system, information to be transmitted is generally available as an electrical signal that may take analog or digital form. Most lightwave systems employ digital signals because of their relative insensitivity to noise. This section describes the two types of signals together with the scheme used to convert an analog signal into a digital one.

I.3.A. Analog and Digital Signals

As shown schematically in Figure I.7, an analog signal (e.g., electric current or voltage) varies continuously with time. Familiar examples include audio and video signals formed when a microphone converts voice or a video camera converts an image into an electrical signal. By contrast, a digital signal takes only a few discrete values. For example, printed text in this book can be thought of as a digital signal because it is composed of about 50 or so symbols (letters, numbers, punctuation marks, etc.).

The most important example of a digital signal is a binary signal for which only two values are possible. In a binary signal, the electric current is either on or off as shown in Figure I.7.

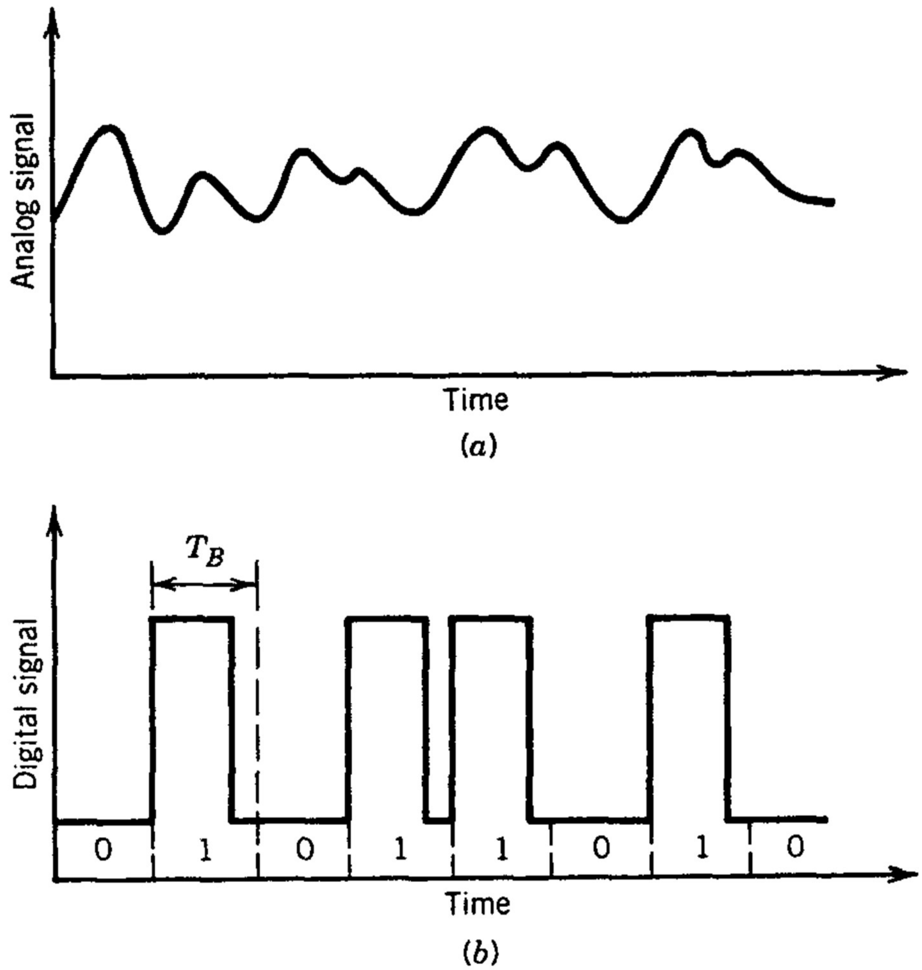

Figure I.7: Analog and digital signals

These two possibilities are called bit 1 and bit 0, respectively. A binary signal thus takes the form of an apparently random sequence of 1 and 0 bits. Each bit lasts for a certain duration T_b, known as the bit period. The bit rate R_b, defined as the number of bits per second, is simply

$$R_b = \frac{1}{T_b} \tag{I.3}$$

Both analog and digital signals are characterized by their bandwidth, which is a measure of the spectral contents of the signal. The signal bandwidth represents the range of frequencies contained within the signal. It is determined mathematically through the Fourier transform $S(f)$ of a time-dependent signal $s(t)$ defined as

$$S(f) = \int_{-\infty}^{\infty} s(t) e^{-j2\pi ft} dt \tag{I.4}$$

I.3.B. Advantages of Digital Format

A lightwave system can transmit information over optical fibers in both the analog and digital formats. However, except for a few special cases, all lightwave systems employ a digital format. The reason behind this choice is related to the relative ease with which a digital signal can be recovered at the receiver even after it has been distorted and corrupted with noise while being transmitted.

Figure I.8 shows schematically why digital signals are relatively immune to noise and distortion in comparison to analog signals. As seen in part (a), the digital signal oscillates between two values, say, 0 and S, for 0 and 1 bits, respectively. Each 1 bit is in the form of a rectangular pulse at the transmitter end. During transmission, the signal is distorted by the dispersive and nonlinear effects occurring within the fiber.

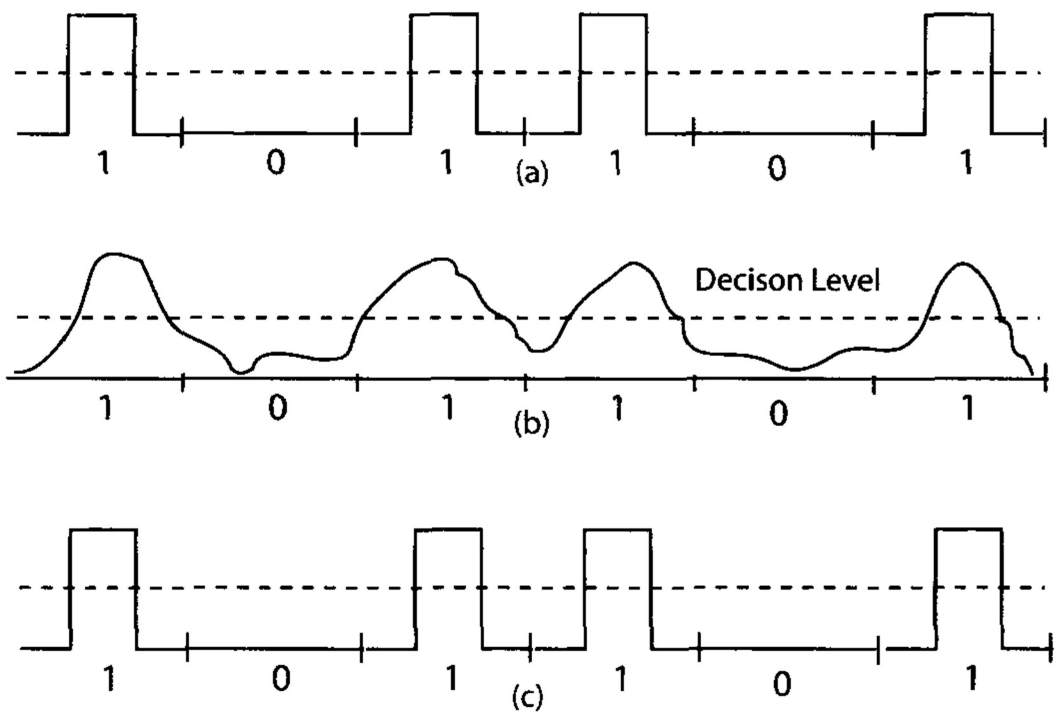

Figure I.8: (a) Transmitted digital signal, (b) distorted and noisy electrical signal at the receiver, and (c) reconstructed digital signal. The thin solid line in the middle shows the decision level.

The addition of noise at the receiver transforms this electrical signal into that shown in part (b). In spite of the signal appearance, the decision circuit at the receiver can still decide between 1 and 0 bits correctly, and reconstruct the original bit sequence as seen in part (c). The reason is related to the fact that the bit identification does not depend on the signal shape but only on whether the signal level exceeds a threshold value at the moment of decision. One can set this threshold value in the middle at $S/2$ to provide the maximum leverage. An error will be made in identifying each 1 bit only if the original value S has dropped to below $S/2$. Similarly, a 0 bit has to acquire an amplitude that is larger than $S/2$ before an error is made.

In contrast, when an analog signal is transmitted through the fiber link, the signal value $s(t)$ at any time t should not change even by 0.1% if one were to ensure fidelity of the transmitted signal because the information is contained in the actual shape of the signal. Mathematically, the SNR of the electrical signal at the receiver should exceed 30 dB for analog signals but, as we shall see in later chapters, it can be lower than 10 dB for digital signals.

The important question one should ask is whether this advantage of digital signals has a price tag attached to it. The answer is related to the signal bandwidth. A digital signal has a much wider bandwidth compared to the analog signal even when the two have the same information content. This feature can be understood from Figure I.8 if we note that the digital signal has much more rapid temporal variations compared with an analog signal.

I.4. Channel Multiplexing

Using pulse code modulation (PCM), a digital voice channel operates at a bit rate of 64 kb/s. Most lightwave systems are capable of transmitting information at a bit rate of more than 1 Gb/s, and the capacity of the fiber channel itself exceeds 10 Tb/s. To utilize the system capacity fully, it is necessary to transmit many channels simultaneously over the same fiber link. This can be accomplished through several multiplexing techniques; the two most common ones are known as time-division multiplexing (TDM) and frequency division multiplexing (FDM). A third scheme, used often for cellular phones and called code-division multiplexing (CDM), can also be used for lightwave systems.

I.4.A. Time-Division Multiplexing

In the case of TDM, bits associated with different channels are interleaved in the time domain to form a composite bit stream. For example, the bit slot is about 15 μs for a single voice channel operating at 64 kb/s. Five such channels can be multiplexed through TDM if bit streams of successive channels are interleaved by delaying them 3 μs. Figure I.9 shows the resulting bit stream schematically at a composite bit rate of 320 kb/s. TDM is readily implemented for digital signals and is commonly used worldwide for telecommunication networks.

The concept of TDM has been used to form digital hierarchies. In North America and Japan, the first level corresponds to multiplexing of 24 voice channels with a composite bit rate of 1.544 Mb/s (hierarchy DS-l), whereas in Europe 30 voice channels are multiplexed, resulting in a composite bit rate of 2.048 Mb/s. The bit rate of the multiplexed signal is slightly larger than the simple product of 64 kb/s with the number of channels because of extra control bits that are added for separating (demultiplexing) the channels at the receiver end. The second-level hierarchy is obtained by multiplexing four DS-1 channels in the time domain. This resulted in a bit rate of 6.312 Mb/s (hierarchy DS-2) for systems commercialized in North America and Japan. At the next level (hierarchy DS-3), seven DS-2 channels were multiplexed through TDM, resulting in a bit rate of close to 45 Mb/s. The first generation of commercial lightwave systems (known as FT-3, short for fiber transmission at DS-3) operated at this bit rate. The same procedure was continued to obtain higher-level hierarchies. For example, at the fifth level of hierarchy, the bit rate was 417 Mb/s for lightwave systems commercialized in North America but 565 Mb/s for systems sold in Europe.

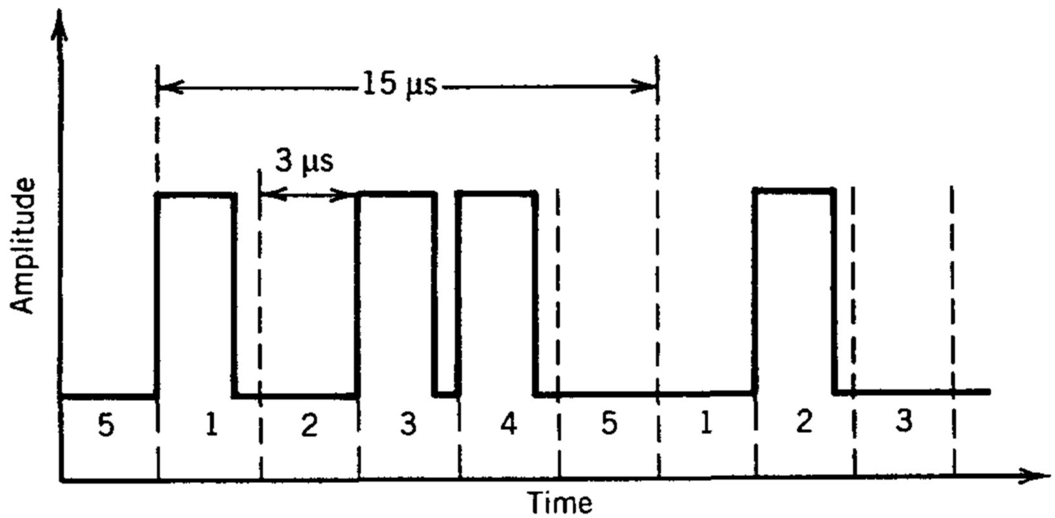

Figure I.9: TDM

The lack of an international standard in the telecommunication industry during the 1980s led to the advent of a new standard, first called the synchronous optical network (SONET) and later termed the synchronous digital hierarchy or SDH. This international standard defines a synchronous frame structure for transmitting TDM digital signals. The basic building block of the SONET has a bit rate of 5 1.84 Mb/s. The corresponding optical signal is referred to as OC- 1, where OC stands for optical carrier. The basic building block of the SDH has a bit rate of 155.52 Mb/s and is referred to as STM-1, where STM stands for a synchronous transport module.

It is important to realize that TDM can be implemented in both the electrical and optical domains. In the optical domain, it is used to combine multiple 10- or 40-Gb/s channels to form an optical bit stream at bit rates exceeding 100 Gb/s. For example, sixteen 10-Gb/s channels, or four 40-Gb/s channels, can be combined through optical TDM for producing bit streams at 160 Gb/s. Optical signal at such high bit rates cannot be generated using an external modulator because of limitations imposed by electronics.

I.4.B. Frequency-Division Multiplexing

In the case of FDM, the channels are spaced apart in the frequency domain but can overlap in the time domain. Each channel is assigned a unique carrier frequency. Moreover, carrier frequencies are spaced more than the channel bandwidth so that channel spectra do not overlap, as seen in Figure I.10. FDM is suitable for both analog and digital signals. It was first developed for radio waves in the beginning of the 20th century and was later adopted by the television industry for broadcasting multiple video channels over microwaves.

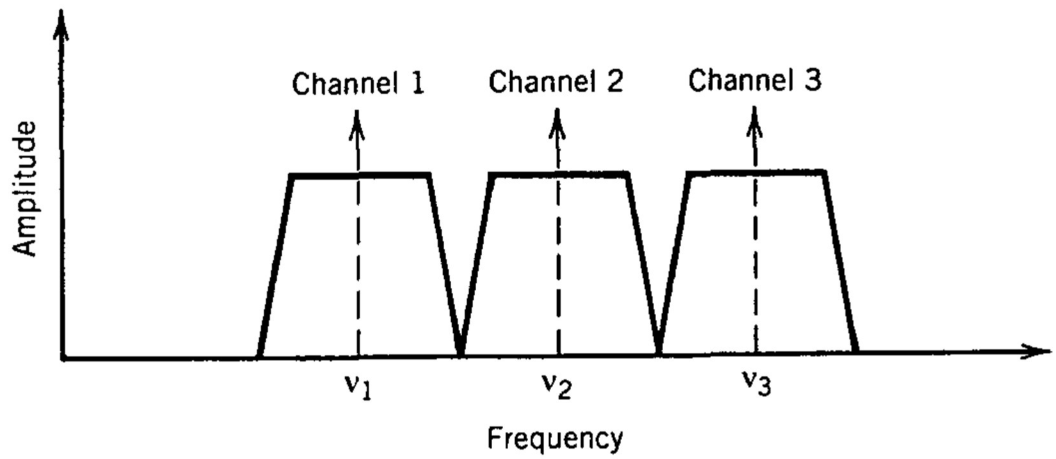

Figure I.10: FDM

FDM can be easily implemented in the optical domain and is commonly referred to as wavelength-division multiplexing (WDM). Each channel is assigned a unique carrier frequency, and an optical source at the precise wavelength corresponding to that frequency is employed within the optical transmitter. The transmitters and receivers used for WDM systems become increasingly complex as the number of WDM channels increases. Figure I.11 shows the basic design of a WDM system schematically. Multiple channels at distinct wavelengths are combined together using a multiplexer and then launched within the same fiber link. At the receiver end, channels are separated using a demultiplexer, typically an optical filter with transmission peaks exactly at the channel wavelengths.

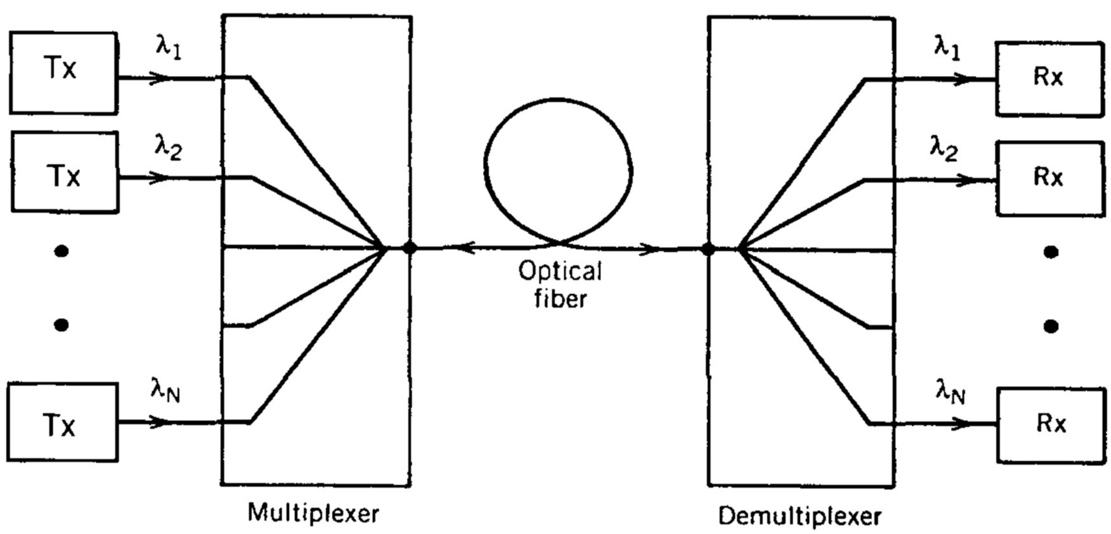

Figure I.11: WDM

WDM systems are often classified as being coarse or dense depending on the channel spacing used. For some applications, only a few channels need to be multiplexed, and channel spacing can be made as large as 1 THz to reduce the system cost. In contrast, dense WDM systems are designed to serve as the backbone of an optical network and often multiplex more than a hundred channels to increase the system capacity. The channel spacing in this case can be as small as 25 GHz for 10-Gb/s channels. The ultimate capacity of a WDM fiber link depends on how closely channels can be packed in the wavelength domain.

I.4.C. Code-Division Multiplexing

Although the TDM and WDM techniques are often employed in practice, both suffer from some drawbacks. The use of TDM to form a single high-speed channel in the optical domain shortens the bit slot to below 10 ps and forces one to use shorter and shorter optical pulses that suffer from dispersive and nonlinear effects. This problem can be solved using the WDM technique but only at the expense of an inefficient utilization of the channel bandwidth. Some of these drawbacks can be overcome by using a multiplexing scheme based on the spread-spectrum technique and is well known in the domain of wireless communications. This scheme is referred to as code-division multiplexing (CDM) because each channel is coded in such a way that its spectrum spreads over a much wider region than occupied by the original signal.

Although spectrum spreading may appear counterintuitive from a spectral point of view, this is not the case because all users share the same spectrum, In fact, CDM is used extensively in cellular systems; as it provides the most flexibility in a multiuser environment. The term code-division multiple access (CDMA) is often employed to emphasize the asynchronous and random nature of multiuser connections. Conceptually, the difference between the WDM, TDM, and CDM can be understood as follows. The WDM and TDM techniques partition, respectively, the channel bandwidth or the time slots among users. In contrast, all users share the entire bandwidth and all time slots in a random fashion in the case of CDM.

I.5. Advantages of optical fiber communication

Enormous potential bandwidth

The optical carrier frequency in the range 10^{13} to 10^{16} Hz (generally in the near infrared around 10^{14} Hz or 10^{5} GHz) yields a far greater potential transmission bandwidth than metallic cable systems or even millimeter wave radio systems.

Small size and weight

Optical fibers have very small diameters which are often no greater than the diameter of a human hair. Hence, even when such fibers are covered with protective coatings they are far smaller and much lighter than corresponding copper cables. This is a tremendous advantage towards the alleviation of duct congestion in cities, as well as allowing for an expansion of signal transmission within mobiles such as aircraft, satellites and even ships.

Electrical isolation

Optical fibers which are fabricated from glass, or sometimes a plastic polymer, are electrical insulators and therefore, unlike their metallic counterparts, they do not exhibit earth loop and interface problems. Furthermore, this property makes optical fiber transmission ideally suited for communication in electrically hazardous environments as the fibers create no arcing or spark hazard at abrasions or short circuits.

Immunity to interference and crosstalk

Optical fibers form a dielectric waveguide and are therefore free from electromagnetic interference (EMI), radio-frequency interference (RFI), or switching transients giving electromagnetic pulses (EMPs). Hence the operation of an optical fiber communication system is unaffected by transmission through an electrically noisy environment and the fiber cable requires no shielding from EMI. The fiber cable is also not susceptible to lightning strikes if used overhead rather than underground. Moreover, it is fairly easy to ensure that there is no optical interference between fibers and hence, unlike communication using electrical conductors, crosstalk is negligible, even when many fibers are cabled together.

Signal security

The light from optical fibers does not radiate significantly and therefore they provide a high degree of signal security. Unlike the situation with copper cables, a transmitted optical signal cannot be obtained from a fiber in a noninvasive manner (i.e. without drawing optical power from the fiber). Therefore, in theory, any attempt to acquire a message signal transmitted optically may be detected. This feature is obviously attractive for military, banking and general data transmission (i.e. computer network) applications.

Low transmission loss

The development of optical fibers over the years has resulted in the production of optical fiber cables which exhibit very low attenuation or transmission loss in comparison with the best copper conductors. Fibers have been fabricated with losses below 0.2 dB/km and this feature has become a major advantage of optical fiber communications. It facilitates the implementation of communication links with extremely wide optical repeater or amplifier spacings, thus reducing both system cost and complexity. Together with the already proven modulation bandwidth capability of fiber cables, this property has provided a totally compelling case for the adoption of optical fiber communications in the majority of long-haul telecommunication applications, replacing not only copper cables, but also satellite communications, as a consequence of the very noticeable delay incurred for voice transmission when using this latter approach.

Ruggedness and flexibility

Although protective coatings are essential, optical fibers may be manufactured with very high tensile strengths. Perhaps surprisingly for a glassy substance, the fibers may also be bent to quite small radii or twisted without damage. Furthermore, cable structures have been developed which have proved flexible, compact and extremely rugged. Taking the size and weight advantage into account, these optical fiber cables are generally superior in terms of storage, transportation, handling and installation to corresponding copper cables, while exhibiting at least comparable strength and durability.

System reliability and ease of maintenance

These features primarily stem from the low-loss property of optical fiber cables which reduces the requirement for intermediate repeaters or line amplifiers to boost the transmitted signal strength.

Hence with fewer optical repeaters or amplifiers, system reliability is generally enhanced in comparison with conventional electrical conductor systems. Furthermore, the reliability of the optical components is no longer a problem with predicted lifetimes of 20 to 30 years being quite common. Both these factors also tend to reduce maintenance time and costs.

Potential low cost

The glass which generally provides the optical fiber transmission medium is made from sand – not a scarce resource. So, in comparison with copper conductors, optical fibers offer the potential for low-cost line communication. Although over recent years this potential has largely been realized in the costs of the optical fiber transmission medium which for bulk purchases has become competitive with copper wires (i.e. twisted pairs), it has not yet been achieved in all the other component areas associated with optical fiber communications. For example, the costs of high-performance semiconductor lasers and detector photodiodes are still relatively high, as well as some of those concerned with the connection technology (demountable connectors, couplers, etc.).

Overall system costs when utilizing optical fiber communication on long-haul links, however, are substantially less than those for equivalent electrical line systems because of the low-loss and wideband properties of the optical transmission medium. The requirement for intermediate repeaters and the associated electronics is reduced, giving a substantial cost advantage. Although this cost benefit gives a net gain for long-haul links, it is not always the case in short-haul applications where the additional cost incurred, due to the electrical–optical conversion (and vice versa), may be a deciding factor. Nevertheless, there are other possible cost advantages in relation to shipping, handling, installation and maintenance, which may prove significant in the system choice.

***

II. Optical Fiber Waveguides

II.1. Introduction

The structure illustrated in Figure II.1, shows a transparent core with a refractive index n_1 surrounded by a transparent cladding of slightly lower refractive index n_2.

$$n_1 > n_2 \tag{II.1}$$

The cladding supports the waveguide structure while also, when sufficiently thick, substantially reducing the radiation loss into the surrounding air. In essence, the light energy travels in both the core and the cladding allowing the associated fields to decay to a negligible value at the cladding–air interface.

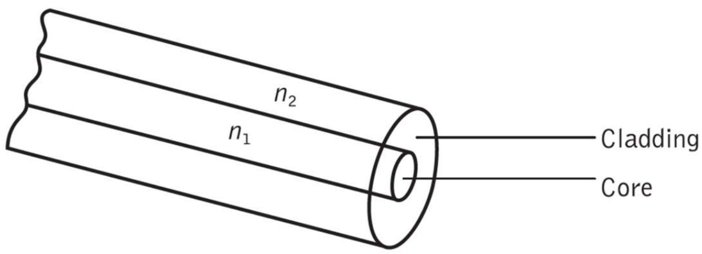

Figure II.1: Optical fiber waveguide

In order to appreciate the transmission mechanism of optical fibers with dimensions approximating to those of a human hair, it is necessary to consider the optical waveguiding of a cylindrical glass fiber. Such a fiber acts as an open optical waveguide, which may be analyzed utilizing simple ray theory. However, the concepts of geometric optics are not sufficient when considering all types of optical fiber, and electromagnetic mode theory must be used to give a complete picture.

II.2. Ray Theory Transmission

II.2.A. Total Internal Reflection

To consider the propagation of light within an optical fiber utilizing the ray theory model it is necessary to take account of the refractive index of the dielectric medium. The refractive index of a medium is defined as the ratio of the velocity of light in a vacuum c to the velocity of light in the medium v.

$$n = \frac{c}{v} \tag{II.2}$$

A ray of light travels more slowly in an optically dense medium than in one that is less dense, and the refractive index gives a measure of this effect. When a ray is incident on the interface between two dielectrics of differing refractive indices (e.g. glass–air), refraction occurs, as illustrated in Figure II.2.

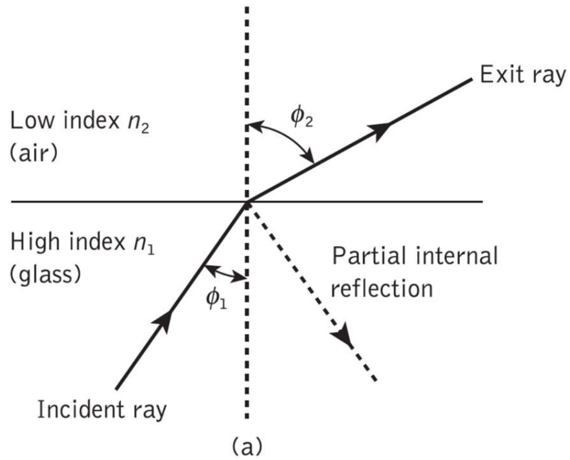

Figure II.2: Refraction

It may be observed that the ray approaching the interface is propagating in a dielectric of refractive index n_1 and is at an angle of incidence ϕ_1 to the normal at the surface of the interface. If the dielectric on the other side of the interface has a refractive index $n_2 < n_1$, then the refraction is such that the ray path in this lower index medium is at an angle of refraction $\phi_2 > \phi_1$. Angles of incidence and refraction are related via Snell's low, given by

$$n_1 \sin\phi_1 = n_2 \sin\phi_2 \tag{II.3}$$

Alternatively, we have

$$\frac{n_1}{n_2} = \frac{\sin\phi_2}{\sin\phi_1} \tag{II.4}$$

It may also be observed in Figure II.2 that a small amount of light is reflected back into the originating dielectric medium (partial internal reflection). When the angle of refraction is 90° and the refracted ray emerges parallel to the interface between the dielectrics, the angle of incidence must be less than 90°. This is the limiting case of refraction and the angle of incidence is now known as the critical angle ϕ_c, as shown in Figure II.3. From (II.4), the value of the critical angle is given by:

$$\sin\phi_c = \frac{n_2}{n_1} \tag{II.5}$$

At angles of incidence greater than the critical angle the light is reflected back into the originating dielectric medium (total internal reflection) with high efficiency (around 99.9%). Hence, it may be observed in Figure II.4 that total internal reflection occurs at the interface between two dielectrics of differing refractive indices when light is incident on the dielectric of lower index from the dielectric of higher index, and the angle of incidence of the ray exceeds the critical value.

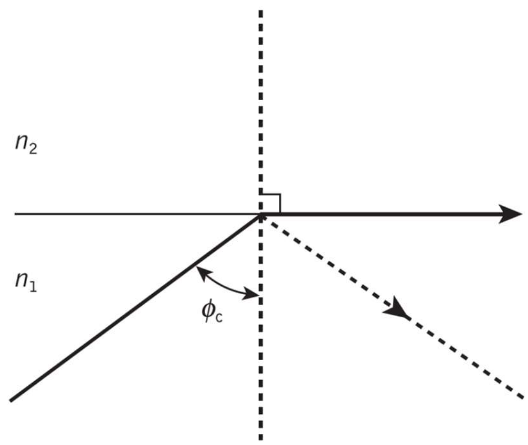

Figure II.3: Critical angle

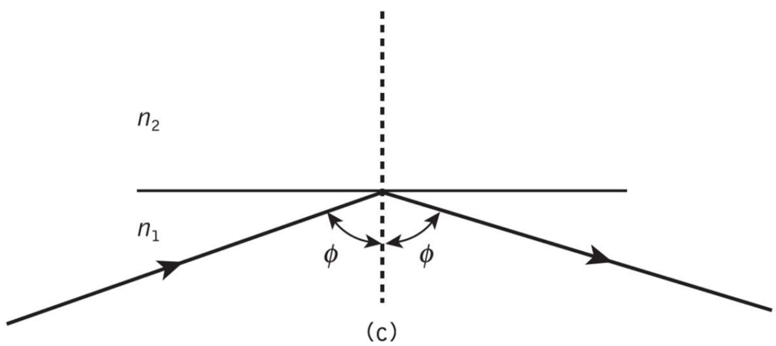

Figure II.4: Total internal reflection

Figure II.5 illustrates the transmission of a light ray in an optical fiber via a series of total internal reflections at the interface of the silica core and the slightly lower refractive index silica cladding. The ray has an angle of incidence ϕ at the interface which is greater than the critical angle and is reflected at the same angle to the normal.

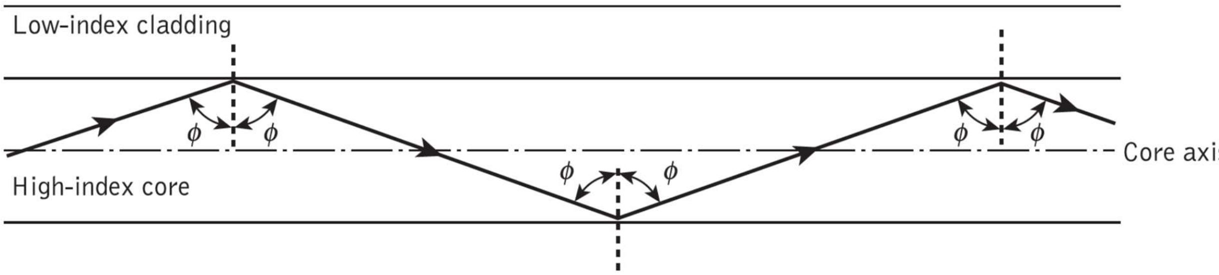

Figure II.5: Light propagation along fiber

The light ray shown in Figure II.5 is known as a meridional ray as it passes through the axis of the fiber core. This type of ray is the simplest to describe and is generally used when illustrating the fundamental transmission properties of optical fibers. It must also be noted that the light transmission illustrated in Figure II.5 assumes a perfect fiber, and that any discontinuities or imperfections at the core-cladding interface would probably result in refraction rather than total internal reflection, with the subsequent loss of the light ray into the cladding.

II.2.B. Acceptance Angle

Having considered the propagation of light in an optical fiber through total internal reflection at the core-cladding interface, it is useful to enlarge upon the geometric optics approach with reference to light rays entering the fiber. Since only rays incident with an angle to the normal greater than ϕ_c at the core-cladding interface are transmitted by total internal reflection, it is clear that not all rays entering the fiber core will continue to be propagated down its length.

The geometry concerned with launching a light ray into an optical fiber is shown in Figure II.6, which illustrates a meridional ray A at the critical angle ϕ_c within the fiber at the core-cladding interface.

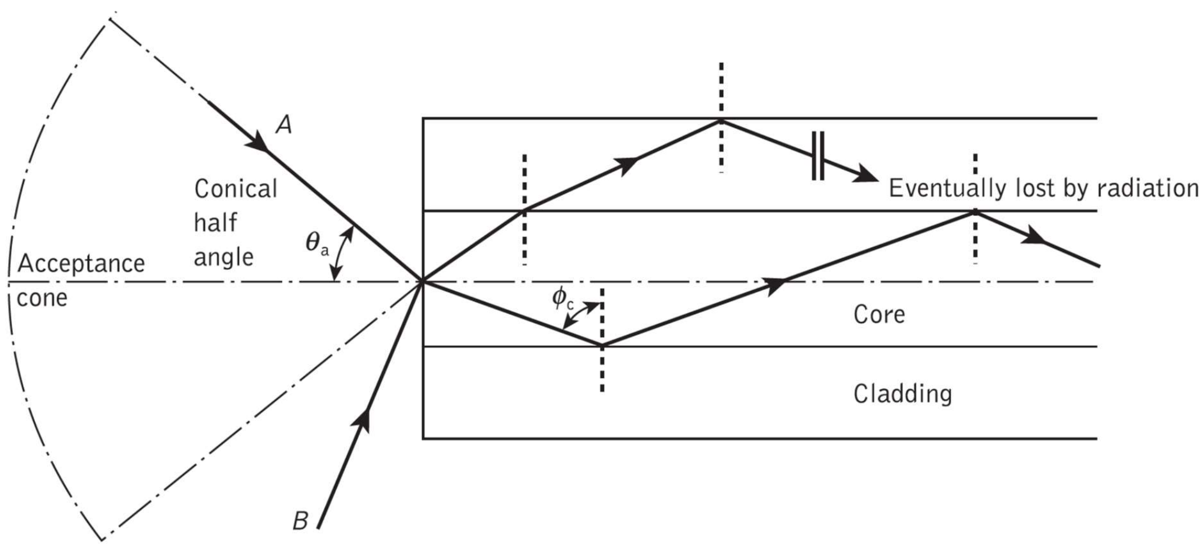

Figure II.6: Acceptance angle

It may be observed that ray A enters the fiber core at an angle θ_a to the fiber axis and is refracted at the air-core interface before transmission to the core-cladding interface at the critical angle. Hence, any rays which are incident into the fiber core at an angle greater than θ_a will be transmitted to the core-cladding interface at an angle less than ϕ_c, and will not be totally internally reflected. This situation is also illustrated in Figure II.6, where the incident ray B at an angle greater than θ_a is refracted into the cladding and eventually lost by radiation. Thus for rays to be transmitted by total internal reflection within the fiber core they must be incident on the fiber core within an acceptance cone defined by the conical half angle θ_a. Hence θ_a is the maximum angle to the axis at which light may enter the fiber in order to be propagated, and is often referred to as the acceptance angle for the fiber.

If the fiber has a regular cross-section (i.e. the core–cladding interfaces are parallel and there are no discontinuities) an incident meridional ray at greater than the critical angle will continue to be reflected and will be transmitted through the fiber. From symmetry considerations it may be noted that the output angle to the axis will be equal to the input angle for the ray, assuming the ray emerges into a medium of the same refractive index from which it was input.

II.2.C. Numerical Aperture

It is possible to continue the ray theory analysis to obtain a relationship between the acceptance angle and the refractive indices of the three media involved, namely the core, cladding and air. This leads to the definition of a more generally used term, the numerical aperture of the fiber. It must be noted that within this analysis, as with the preceding discussion of acceptance angle, we are concerned with meridional rays within the fiber.

Figure II.7 shows a light ray incident on the fiber core at an angle θ_1 to the fiber axis which is less than the acceptance angle for the fiber θ_a. The ray enters the fiber from a medium (air) of refractive index n_0, and the fiber core has a refractive index n_1, which is slightly greater than the cladding refractive index n_2.

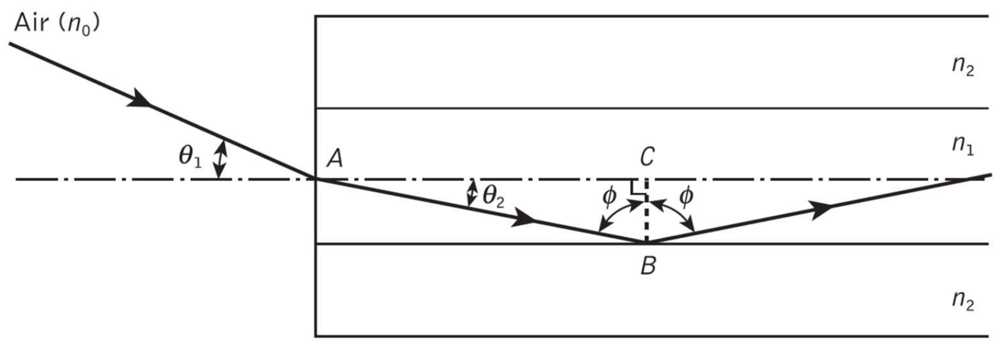

Figure II.7: Numerical aperture

Assuming the entrance face at the fiber core to be normal to the axis, then considering the refraction at the air–core interface and using Snell's law given by

$$n_0 \sin\theta_1 = n_1 \sin\theta_2 \tag{II.6}$$

Note that in Figure II.7,

$$\phi = \frac{\pi}{2} - \theta_2 \tag{II.7}$$

Note that ϕ is greater than the critical angle at the core–cladding interface. Substituting (II.7) into (II.6) yields

$$\begin{aligned} n_0 \sin\theta_1 &= n_1 \cos\phi \\ &= n_1\sqrt{1-\sin^2\phi} \end{aligned} \tag{II.8}$$

When the limiting case for total internal reflection is considered, ϕ becomes equal to the critical angle for the core-cladding interface and is given by (II.5). Also in this limiting case θ_1 becomes the acceptance angle for the fiber θ_a. Combining these limiting cases into (II.8) gives

$$\begin{aligned} n_0 \sin\theta_a &= \sqrt{n_1^2 - n_1^2 \sin^2\phi_c} \\ &= \sqrt{n_1^2 - n_2^2} \end{aligned} \tag{II.9}$$

Numerical aperture (NA) is defined as

$$\begin{aligned} NA &= n_0 \sin\theta_a \\ &= \sqrt{n_1^2 - n_2^2} \end{aligned} \tag{II.10}$$

Let the relative refractive index difference be defined as

$$\Delta = \frac{n_1^2 - n_2^2}{2n_1^2} \tag{II.11}$$

When $\Delta << 1$, it can be approximated as

$$\Delta \approx \frac{n_1 - n_2}{n_1} \tag{II.12}$$

Combining (II.10) and (II.11) produces

$$NA = n_1\sqrt{2\Delta} \tag{II.13}$$

The relationships given in (II.10) and (II.13) for the numerical aperture are a very useful measure of the light-collecting ability of a fiber. They are independent of the fiber core diameter and will hold for diameters as small as 8 μm. However, for smaller diameters they break down as the geometric optics approach is invalid. This is because the ray theory model is only a partial description of the character of light. It describes the direction a plane wave component takes in the fiber but does not take into account interference between such components. When interference phenomena are considered it is found that only rays with certain discrete characteristics propagate in the fiber core. Thus the fiber will only support a discrete number of guided modes. This becomes critical in small-core-diameter fibers which only support one or a few modes. Hence electromagnetic mode theory must be applied in these cases.

Example II.1

A silica optical fiber with a core diameter large enough to be considered by ray theory analysis has a core refractive index of 1.50 and a cladding refractive index of 1.47. determine

a. the critical angle at the core-cladding interface
b. the numerical aperture for the fiber
c. the acceptance angle in air for the fiber

Solution

a. $\phi_c = \sin^{-1}\left(\frac{n_2}{n_1}\right) = \sin^{-1}\left(\frac{1.47}{1.5}\right) = 78.5^\circ$

b. $NA = \sqrt{n_1^2 - n_2^2} = 0.3$

c. $\theta_a = \sin^{-1} NA = \sin^{-1}(0.3) = 17.4^\circ$

Example II.2

A typical relative refractive index difference for an optical fiber designed for long-distance transmission is 1%. Estimate the NA and the solid acceptance angle in air for the fiber when the core index is 1.46. Further, calculate the critical angle at the core-cladding interface within the fiber. It may be assumed that the concepts of geometric optics hold for the fiber.

Solution

$\Delta = 0.01$.

$NA = n_1\sqrt{2\Delta} = 0.21$.

For small angles the solid acceptance angle in air ζ is given by

$$\zeta \approx \pi\theta_a^2 = \pi \sin^2\theta_a \approx \pi(NA)^2 = 0.13 \text{ rad}.$$

$$\Delta \approx \frac{n_1 - n_2}{n_1} = 1 - \frac{n_2}{n_1} \Rightarrow \frac{n_2}{n_1} = 1 - \Delta = 0.99 \Rightarrow n_2 = 1.4454.$$

$$\phi_c = \sin^{-1}\left(\frac{n_2}{n_2}\right) = \sin^{-1}(0.99) = 81.9^\circ.$$

II.3. Optical Fiber Types and Classifications

The size of an optical waveguide must be comparable to the wavelength of light. Therefore, the diameter of optical fibers are typically in the order of few to tens of micrometers. The core of an optical fiber must have a slightly larger index of refraction compared to the cladding. The transition of the index of refraction from the core to cladding can take many forms, and several optical properties of the fiber are determined by the radial profile of the index of refraction.

II.3.A. Single-Mode Step-Index Fiber

Figure II.8 shows the refractive index profile of a single-mode step-index fiber.

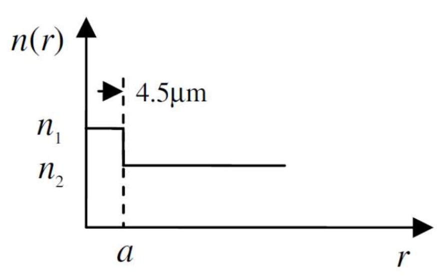

Figure II.8: Single-mode step-index profile

Single-mode fibers have a very narrow core diameter, usually in the range of 9 µm.

II.3.B. Multimode Step-Index Fiber

Figure II.9 shows the refractive index profile of a multimode step-index fiber.

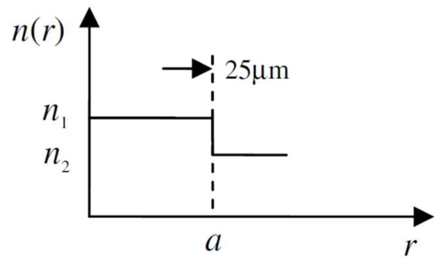

Figure II.9: Single-mode graded index profile

Multimode fibers have much wider core diameters, compared to single-mode fibers. Multimode fibers have core diameters that are usually in the range of 50 μm.

II.3.C. Multimode Graded Index Fiber

Figure II.10 shows the refractive index profile of a multimode graded index fiber.

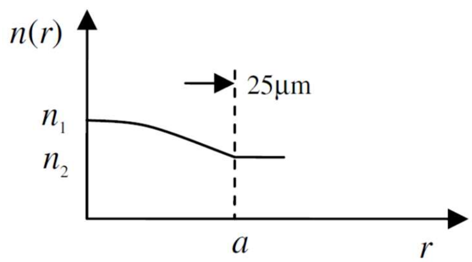

Figure II.10: Multimode graded index profile

Note that

$$n(0) = n_1 \tag{II.14}$$

$$n(a) = n_2 \tag{II.15}$$

A graded index profile can follow a variety of mathematical expressions. An important example graded index profile is given by

$$n(r) = n_2 + (n_1 - n_2)\left[1 - \left(\frac{r}{a}\right)^{\gamma}\right] \tag{II.16}$$

where γ is a power law exponent that determines the shape of the profile. When $\gamma = 2$ we have a parabolic graded index profile.

II.4. Electromagnetic Mode Theory for Optical Propagation

II.4.A. Optical Waveguides

An optical waveguide must be made from a transparent material. In general the materials used in the construction of optical fibers include plastics and glasses. Therefore, optical fibers can be divided into glass fibers and plastic optical fibers (POFs). Optical attenuation in plastics is much higher than the attenuation in glasses.

Plastic fibers are mechanically sturdy and easier to manufacture. As a result, plastic fibers can provide an economic solution for very short-distance applications. On the other hand, glasses are excellent candidate materials for optical waveguides because of their very low loss. As a result, virtually all communication fibers are glass based. The most common glass used in fabrication of fibers is silica (SiO_2). In particular, the index of refraction of silica can be modified through doping. Dopants such as P_2O_5 and GeO_2 slightly increase the index of refraction of silica, while dopants like B_2O_3 reduce the index of refraction. With these materials, the achievable loss in optical fibers reduced from 20 dB/km in 1970 to almost 0.2 dB/km (at 1550 nm) in 1979. This is close to the theoretical limit of 0.15dB/km.

II.4.B. Electromagnetic Waves

In order to obtain an improved model for the propagation of light in an optical fiber, electromagnetic wave theory must be considered. The basis for the study of electromagnetic wave propagation is provided by Maxwell's equations. For a medium with zero conductivity these vector relationships may be written in terms of the electric field $\vec{E}$, magnetic field $\vec{H}$, electric flux density $\vec{D}$ and magnetic flux density $\vec{B}$ as the curl equations

$$\vec{\nabla}\times\vec{E} = -\frac{\partial\vec{B}}{\partial t} \tag{II.17}$$

$$\vec{\nabla}\times\vec{H} = \frac{\partial\vec{D}}{\partial t} \tag{II.18}$$

We also have the divergence conditions

$$\vec{\nabla}\cdot\vec{D} = 0 \text{ (no free charges)} \tag{II.19}$$

$$\vec{\nabla}\cdot\vec{B} = 0 \text{ (no free poles)} \tag{II.20}$$

The four field vectors are related by the relations

$$\vec{D} = \varepsilon\vec{E} \tag{II.21}$$

$$\vec{B} = \mu\vec{H} \tag{II.22}$$

where ε is the dielectric permittivity and μ is the magnetic permeability of the medium.

Substituting for $\vec{D}$ and $\vec{B}$ and taking the curl of (II.17) and (II.18) gives

$$\vec{\nabla}\times(\vec{\nabla}\times\vec{E})=-\mu\varepsilon\frac{\partial^2\vec{E}}{\partial t^2} \tag{II.23}$$

$$\vec{\nabla}\times(\vec{\nabla}\times\vec{H})=-\mu\varepsilon\frac{\partial^2\vec{H}}{\partial t^2} \tag{II.24}$$

Note that we have used the vector identity

$$\vec{\nabla}\times(\vec{\nabla}\times\vec{Y})=\vec{\nabla}(\vec{\nabla}\cdot\vec{Y})-\overrightarrow{\nabla^2}(\vec{Y}) \tag{II.25}$$

Using (II.19), (II.20) and (II.25), we obtain the nondispersive wave equations

$$\overrightarrow{\nabla^2}(\vec{E})=\mu\varepsilon\frac{\partial^2\vec{E}}{\partial t^2} \tag{II.26}$$

$$\overrightarrow{\nabla^2}(\vec{H})=\mu\varepsilon\frac{\partial^2\vec{H}}{\partial t^2} \tag{II.27}$$

Let the phase velocity be defined as

$$\begin{aligned} v_p &= \frac{1}{\sqrt{\mu\varepsilon}} \\ &= \frac{1}{\sqrt{\mu_r\mu_0\varepsilon_r\varepsilon_0}} \\ &= \frac{c}{n} \end{aligned} \tag{II.28}$$

where μ_r and ε_r are the relative permeability and permittivity for the dielectric medium and μ_0 and ε_0 are the permeability and permittivity of free space. The velocity of light in free space is given by

$$c=\frac{1}{\sqrt{\mu_0\varepsilon_0}} \tag{II.29}$$

Assuming the material in each layer is non-magnetic and isotropic, then ε is a scalar and

$$\mu_r=1 \tag{II.30}$$

As a result,

$$n = \sqrt{\varepsilon_r} \tag{II.31}$$

For rectangular Cartesian and cylindrical polar coordinates the above wave equations hold for each component of the field vector, every component satisfying the scalar wave equation

$$\nabla^2 \psi = \frac{1}{v_p^2} \frac{\partial^2 \psi}{\partial t^2} \tag{II.32}$$

In planar waveguides, described by rectangular Cartesian coordinates (x , y , z), or circular fibers, described by cylindrical polar coordinates (r , θ , z), are considered, then the Laplacian operator takes the forms

$$\nabla^2 \psi = \frac{\partial^2}{\partial x^2}\psi + \frac{\partial^2}{\partial y^2}\psi + \frac{\partial^2}{\partial z^2}\psi \tag{II.33}$$

$$\nabla^2 \psi = \frac{\partial^2}{\partial r^2}\psi + \frac{1}{r}\frac{\partial}{\partial r}\psi + \frac{1}{r^2}\frac{\partial^2}{\partial \theta^2}\psi + \frac{\partial^2}{\partial z^2}\psi \tag{II.34}$$

It is necessary to consider both these forms for a complete treatment of optical propagation in the fiber, although many of the properties of interest may be dealt with using Cartesian coordinates.

The basic solution of the wave equation is a sinusoidal wave, the most important form of which is a uniform plane wave given by

$$\psi = \psi_0 e^{j(\omega t - \vec{k}\cdot\vec{r})} \tag{II.35}$$

where ω is the angular frequency of the field, t is the time, $\vec{k}$ is the propagation vector which gives the direction of propagation and the rate of change of phase with distance, while the components of $\vec{r}$ specify the coordinate point at which the field is observed.

When λ is the optical wavelength in a vacuum, the magnitude of the propagation vector or the vacuum phase propagation constant is given by

$$\begin{aligned} k &= \left|\vec{k}\right| \\ &= \frac{2\pi}{\lambda} \\ &= \frac{2\pi f}{c} \\ &= \frac{\omega}{c} \\ &= \omega\sqrt{\mu_0 \varepsilon_0} \end{aligned} \tag{II.36}$$

It should be noted that in this case k is also referred to as the free space wave number.

II.4.C. Modes in a Planar Guide

The planar guide is the simplest form of optical waveguide. We may assume it consists of a slab of dielectric with refractive index n_1 sandwiched between two regions of lower refractive index $n_2 < n_1$. In order to obtain an improved model for optical propagation (compared to ray theory) it is useful to consider the interference of plane wave components within this dielectric waveguide.

The conceptual transition from ray to wave theory may be aided by consideration of a plane monochromatic wave propagating in the direction of the ray path within the guide (see Figure II.11). As the refractive index within the guide is n_1, the optical wavelength in this region is reduced to λ/n_1, while the propagation constant becomes $n_1 k$. When θ is the angle between the wave propagation vector or the equivalent ray and the guide axis, the plane wave can be resolved into two component plane waves propagating in the z and x directions, as shown in Figure II.11.

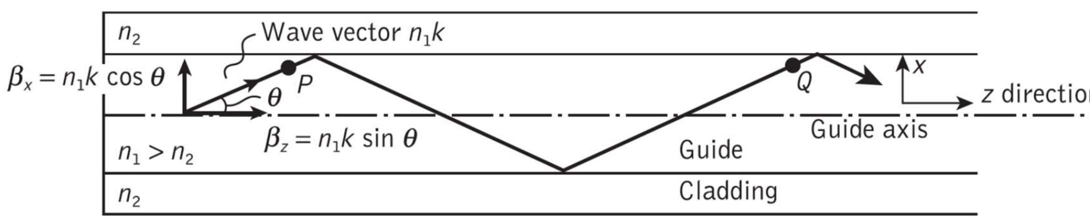

Figure II.11: Planar waveguide

The components of the phase propagation constant in the z and x directions are given by

$$\beta_z = n_1 k \cos\theta \tag{II.37}$$

$$\beta_x = n_1 k \sin\theta \tag{II.38}$$

Consider a wave that is incident on the guide-cladding interface of a planar dielectric waveguide, as shown in Figure II.12. The wave vectors of the incident, transmitted and reflected waves are indicated (solid arrowed lines) together with their components in the z and x directions (dashed arrowed lines). Note that $\phi_1 = \pi/2 - \theta$. Note also that a component of the wave energy is shown to be transmitted through the interface into the cladding.

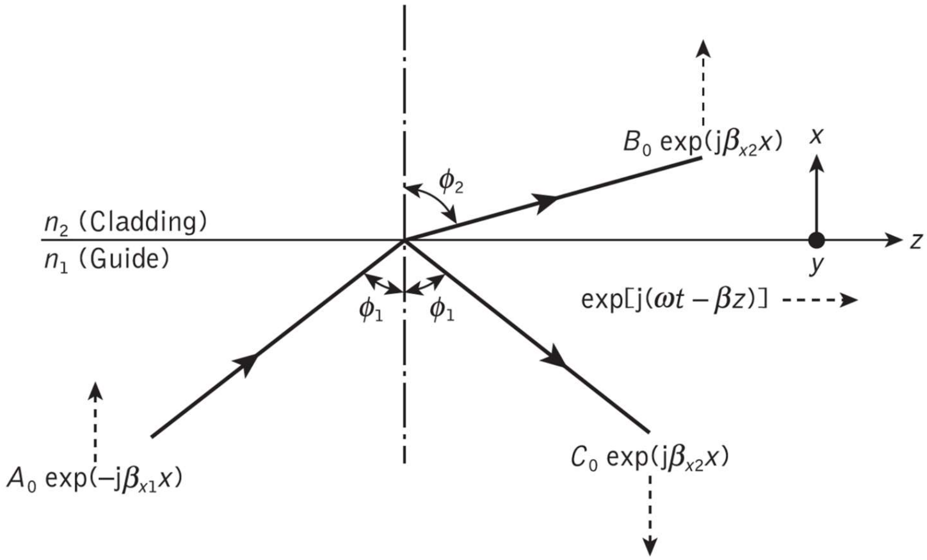

Figure II.12: Reflection phase shift

Correct $C_0 e^{j\beta_{x2}x}$ to $C_0 e^{j\beta_{x1}x}$

From (II.26), the wave equation in Cartesian coordinates for the electric field in a lossless medium is

$$\nabla^2 \vec{E} = \mu\varepsilon \frac{\partial^2 \vec{E}}{\partial t^2} \tag{II.39}$$

As the guide–cladding interface lies in the $y-z$ plane and the wave is incident in the $x-z$ plane onto the interface, then $\partial/\partial y$ may be assumed to be zero. The wave propagation in the z direction may be described by $\exp[j(\omega t - \beta z]$. Thus the three waves in the waveguide: the incident wave, the transmitted wave and the reflected wave, with amplitudes A_0, B_0 and C_0, respectively, will have the forms

$$A = A_0 e^{-j\beta_{x1}x} e^{j(\omega t - \beta_z z)} \tag{II.40}$$

$$B = B_0 e^{-j\beta_{x2}x} e^{j(\omega t - \beta_z z)} \tag{II.41}$$

$$C = C_0 e^{j\beta_{x1}x} e^{j(\omega t - \beta_z z)} \tag{II.42}$$

Equation (II.32) can be rewritten in the form

$$\nabla^2 \psi = \frac{n^2}{c^2} \frac{\partial^2 \psi}{\partial t^2} \tag{II.43}$$

Using (II.35), it can be seen that

$$\frac{\partial^2 \psi}{\partial t^2} = -\omega^2 \psi \qquad \text{(II.44)}$$

From (II.36), we have $\omega = ck$, resulting in

$$\frac{\partial^2 \psi}{\partial t^2} = -c^2 k^2 \psi \qquad \text{(II.45)}$$

Substituting (II.45) into (II.43), we get

$$\nabla^2 \psi = -n^2 k^2 \psi \qquad \text{(II.46)}$$

Rearranging the terms in (II.46) results in

$$\nabla^2 \psi + n^2 k^2 \psi = 0 \qquad \text{(II.47)}$$

We may simplify (II.47) by assuming that the waveguide is uniform in the y direction and that it extends to infinity in the y direction. This also allows us to assume that the field is uniform in this direction. Therefore,

$$\frac{\partial \psi}{\partial y} = 0 \qquad \text{(II.48)}$$

Since from (II.35) it can be concluded that the field dependence on z follows the form $e^{-j\beta z}$, it follows that

$$\frac{\partial^2 \psi}{\partial z^2} = -\beta^2 \psi \qquad \text{(II.49)}$$

Substituting (II.48) and (II.49) into (II.47), we get

$$\frac{d^2 \psi}{dx^2} + (n^2 k^2 - \beta^2)\psi = 0 \qquad \text{(II.50)}$$

Equation (II.50) is known as the Helmholtz equation. The equation is a second order ordinary differential equation, and the solution is a function of only x. Let

$$\beta = n_{\text{eff}} k \qquad \text{(II.51)}$$

where n_{eff} is the effective refractive index. The total field is a superposition of a transverse electric (TE) part (with components E_y, H_x, H_z) and a transverse magnetic (TM) part (with components H_y, E_x, E_z).

Consider the following structure.

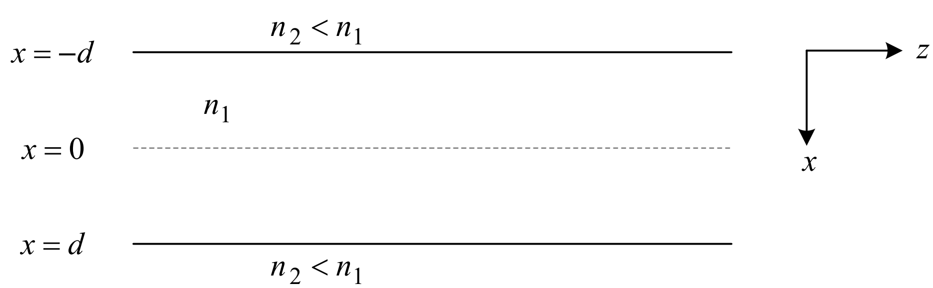

Figure II.13: Planar waveguide

II.4.D. Transverse Electric Guided Modes

Note that for TE modes, $E_x = E_z = 0$. Using (II.35) with $\vec{k} \cdot \vec{r} = \beta z$ in (II.50) yields

$$\frac{d^2}{dx^2}\left[\psi_0 e^{j(\omega t - \beta z)}\right] + (n^2 k^2 - \beta^2)\left[\psi_0 e^{j(\omega t - \beta z)}\right] = 0 \qquad \text{(II.52)}$$

This simplifies to

$$\frac{d^2 \psi_0}{dx^2} + (n^2 k^2 - \beta^2)\psi_0 = 0 \qquad \text{(II.53)}$$

Applying (II.53) to E_y yields

$$\frac{d^2 E_{0y}}{dx^2} - p^2 E_{0y} = 0, \quad x \le -d \ \text{ or } x \ge d \qquad \text{(II.54)}$$

where

$$p^2 = \beta^2 - n_2^2 k^2 \qquad \text{(II.55)}$$

$$\frac{d^2 E_{0y}}{dx^2} + q^2 E_{0y} = 0, \quad -d \le x \le d \qquad \text{(II.56)}$$

where

$$q^2 = n_1^2 k^2 - \beta^2 \tag{II.57}$$

For guided modes, the power is required to be largely confined to the central region of the guide (the n_1 region), with as little power as possible escaping to the outer regions (the n_2 regions). Based on (II.56), the power confinement requirement can be satisfied if E_y is assumed to be oscillatory in the inner region. The field in the outer regions can be assumed to follow a decaying exponential shape.

For even modes we could use

$$E_{0y} = \begin{cases} A\cos(qd)e^{p(d+x)}, & x \le -d \\ A\cos(qx), & -d \le x \le d \\ A\cos(qd)e^{(d-x)p}, & x \ge d \end{cases} \tag{II.58}$$

Note that E_{0y} is tangential to the waveguide interfaces, and it is continuous at both $x = d$ and $x = -d$.

From (II.17) and (II.22),

$$H_{0x} = -\frac{\beta}{\omega\mu_0} E_{0y} \tag{II.59}$$

$$H_{0z} = -\frac{j}{\omega\mu_0} \frac{dE_{0y}}{dx} \tag{II.60}$$

Since H_{0z} is also tangential to the waveguide interfaces, and it must be continuous at both $x = d$ and $x = -d$. Substituting (II.58) into (II.60) yields

$$H_{0z} = -\frac{j}{\omega\mu_0} \begin{cases} pA\cos(qd)e^{p(d+x)}, & x \le -d \\ -qA\sin(qx), & -d \le x \le d \\ -pA\cos(qd)e^{(d-x)p}, & x \ge d \end{cases} \tag{II.61}$$

At $x = \pm d$ we get

$$\begin{aligned} pA\cos(qd) &= qA\sin(qd) \\ pd\cos(qd) &= qd\sin(qd) \end{aligned} \tag{II.62}$$

Equation (II.62) can be rewritten as

$$qd\tan(qd) = pd \tag{II.63}$$

For odd modes we could use

$$E_{0y} = \begin{cases} -A\sin(qd)e^{p(d+x)}, & x \le -d \\ A\sin(qx), & -d \le x \le d \\ A\sin(qd)e^{(d-x)p}, & x \ge d \end{cases} \tag{II.64}$$

$$H_{0z} = -\frac{j}{\omega\mu_0} \begin{cases} -pA\sin(qd)e^{p(d+x)}, & x \le -d \\ qA\cos(qx), & -d \le x \le d \\ -pA\sin(qd)e^{(d-x)p}, & x \ge d \end{cases} \tag{II.65}$$

At $x = \pm d$ we get

$$qd\cot(qd) = -pd \tag{II.66}$$

Equations (II.63) and (II.66) are known as the eigenvalue equations for the TE modes of the dielectric slab waveguide. Equations (II.63) and (II.66) represent an implicit relationship which involves the wavelength, the refractive indices of the layers, and the core thickness as known quantities. The only unknown quantity is the propagation constant.

Only certain values of β can satisfy the eigenvalue equation. This means that the waveguide can support a discrete number of guided modes. Allowed values of β can be found using numerical and graphical techniques.

Adding (II.55) and (II.57) yields

$$p^2 + q^2 = (n_1^2 - n_2^2)k^2 \tag{II.67}$$

Multiply both sides of (II.67) by d^2 to get

$$\begin{aligned}(pd)^2 + (qd)^2 &= (n_1^2 - n_2^2)k^2d^2 \\ &= V^2\end{aligned} \tag{II.68}$$

The quantity V in (II.68) is known as the normalized frequency variable. Note that (II.68) represents a circle of radius

$$\begin{aligned}V &= kd\sqrt{n_1^2 - n_2^2} \\ &= \frac{2\pi}{\lambda}d\sqrt{n_1^2 - n_2^2}\end{aligned} \tag{II.69}$$

Therefore, pairs (pd, qd) must be located on the circumference of a circle with radius V.

Example II.3

A planar waveguide has $\lambda = 0.85$ µm, $n_1 = 1.49$, $n_2 = 1.48$ and $d = 50$ µm. Determine the normalized frequency variable.

$$V = \frac{2\pi \times 50 \times 10^{-6}}{0.85 \times 10^{-6}} \sqrt{1.49^2 - 1.48^2} = 63.7 .$$

If $q = 0.9 \times 10^6 \text{ m}^{-1}$ is an eigenvalue, determine p and β.

$qd = 45$. $(pd)^2 = V^2 - (qd)^2 \Rightarrow p = 0.902 \times 10^6 \text{ m}^{-1}$.

$\beta^2 = n_1^2 k^2 - q^2 \Rightarrow \beta = 10.98 \times 10^6 \text{ m}^{-1}$.

Example II.4

A planar waveguide has $\omega = 2 \times 10^{15}$ rad/s, $n_1 = 1.505$, $n_2 = 1.495$ and $d = 5$ µm. Determine the propagation constants for each propagating mode.

$V = 5.7735$. $0 < qd < 5.7735$. $V^2 = 33.333$.

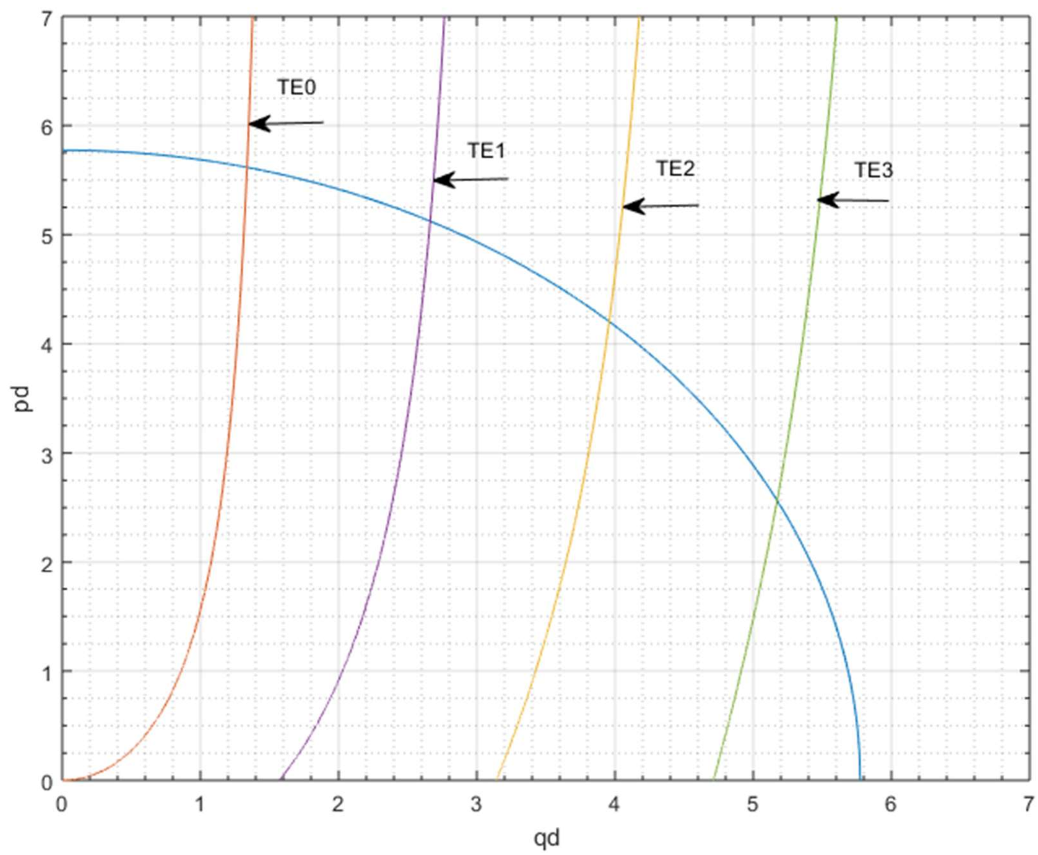

Figure II.14: Even and odd TE modes

TE_0: $pd = 5.6165$ $p = 1.1233 \times 10^{6}\ \mathrm{m}^{-1}$ $qd = 1.3371$ $q = 0.2674 \times 10^{6}\ \mathrm{m}^{-1}$

TE_1: $pd = 5.123$ $p = 1.0246 \times 10^{6}\ \mathrm{m}^{-1}$ $qd = 2.6623$ $q = 0.5325 \times 10^{6}\ \mathrm{m}^{-1}$

TE_2: $pd = 4.204$ $p = 0.8408 \times 10^{6}\ \mathrm{m}^{-1}$ $qd = 3.9572$ $q = 0.7914 \times 10^{6}\ \mathrm{m}^{-1}$

TE_3: $pd = 2.5645$ $p = 0.5129 \times 10^{6}\ \mathrm{m}^{-1}$ $qd = 5.1727$ $q = 1.0345 \times 10^{6}\ \mathrm{m}^{-1}$

$$\beta = \left.\begin{matrix} 9.99642 \\ 9.98581 \\ 9.96863 \\ 9.94634 \end{matrix}\right\} \times 10^{6}\ \mathrm{m}^{-1}$$

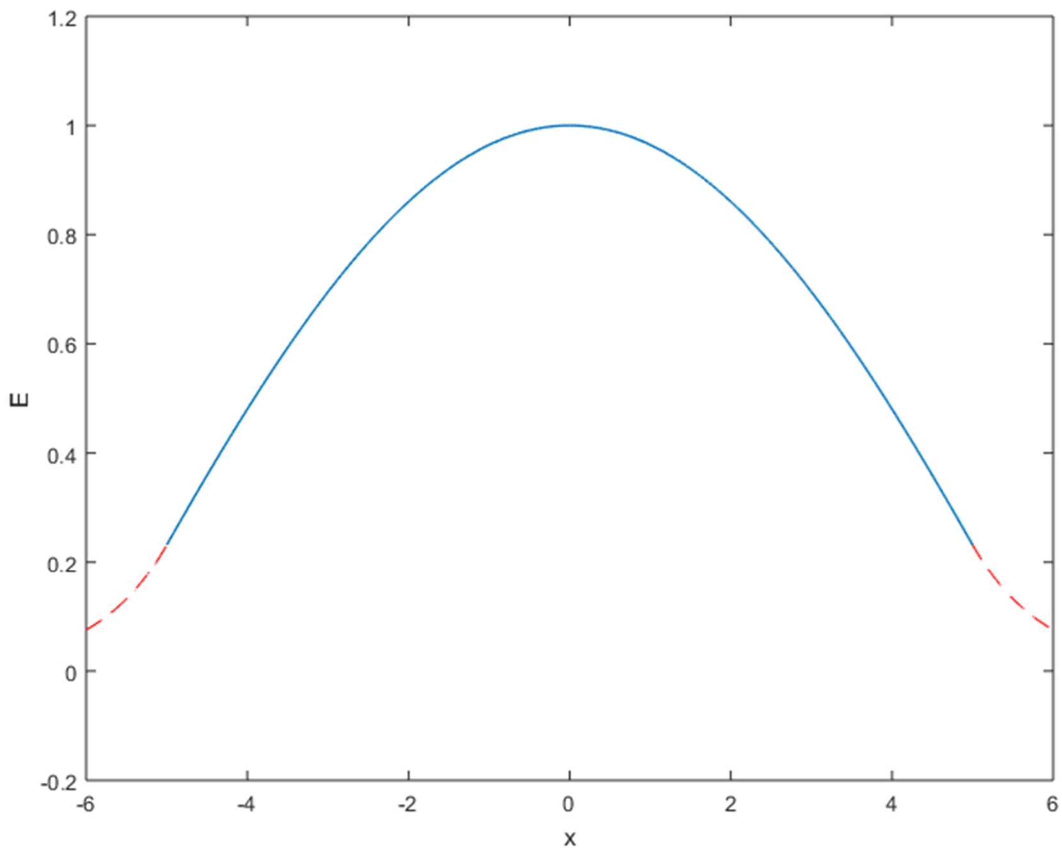

Figure II.15: TE_0 mode

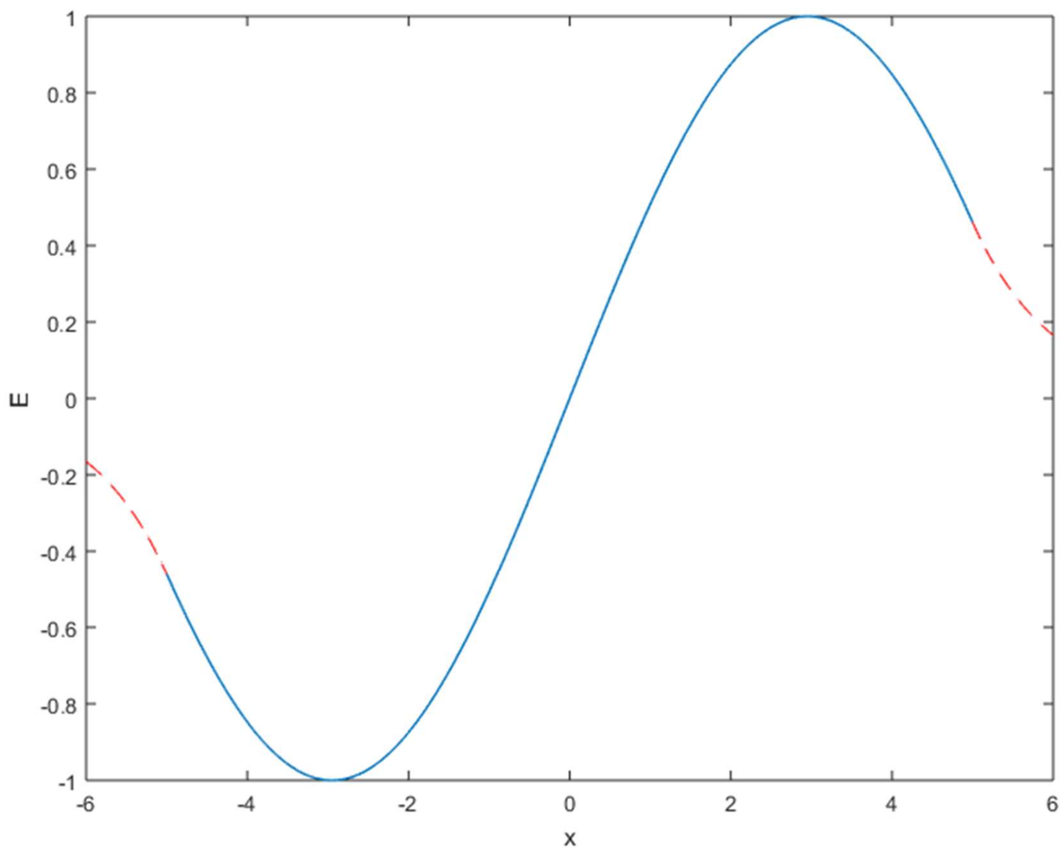

Figure II.16: TE_1 mode

II.4.E. Transverse Magnetic Guided Modes

The consider field components in this case are H_y, E_x, E_z. Note that for TM modes, $H_x = H_z = 0$. Using (II.35) with $\vec{k} \cdot \vec{r} = \beta z$ in (II.50) yields

$$\frac{d^2}{dx^2}\left[\psi_0 e^{j(\omega t - \beta z)}\right] + (n^2 k^2 - \beta^2)\left[\psi_0 e^{j(\omega t - \beta z)}\right] = 0 \tag{II.70}$$

This simplifies to

$$\frac{d^2 \psi_0}{dx^2} + (n^2 k^2 - \beta^2)\psi_0 = 0 \tag{II.71}$$

Applying (II.71) to H_y yields

$$\frac{d^2 H_{0y}}{dx^2} - p^2 H_{0y} = 0, \quad x \le -d \text{ or } x \ge d \tag{II.72}$$

where

$$p^2 = \beta^2 - n_2^2 k^2 \tag{II.73}$$

$$\frac{d^2 E_{0y}}{dx^2} + q^2 E_{0y} = 0, \quad -d \le x \le d \tag{II.74}$$

where

$$q^2 = n_1^2 k^2 - \beta^2 \tag{II.75}$$

From (II.18) and (II.21),

$$E_{0x} = \frac{\beta}{\omega\varepsilon} H_{0y} \tag{II.76}$$

$$E_{0z} = \frac{j}{\omega\varepsilon} \frac{dH_{0y}}{dx} \tag{II.77}$$

For even modes we could use

$$H_{0y} = \begin{cases} C\cos(qd)e^{p(d+x)}, & x \le -d \\ C\cos(qx), & -d \le x \le d \\ C\cos(qd)e^{(d-x)p}, & x \ge d \end{cases} \tag{II.78}$$

Note that H_{0y} is tangential to the waveguide interfaces, and it is continuous at both $x = d$ and $x = -d$.

Since E_{0z} is also tangential to the waveguide interfaces, and it must be continuous at both $x = d$ and $x = -d$. Substituting (II.78) into (II.77) yields

$$E_{0z} = \frac{j}{\omega\varepsilon_0} \begin{cases} \frac{p}{n_2^2} C\cos(qd)e^{p(d+x)}, & x \le -d \\ -\frac{q}{n_1^2} C\sin(qx), & -d \le x \le d \\ -\frac{p}{n_2^2} C\cos(qd)e^{(d-x)p}, & x \ge d \end{cases} \tag{II.79}$$

At $x = \pm d$ we get

$$\frac{n_2^2}{n_1^2} qd \tan(qd) = pd \tag{II.80}$$

For odd modes we could use

$$H_{0y} = \begin{cases} -C\sin(qd)e^{p(d+x)}, & x \le -d \\ C\sin(qx), & -d \le x \le d \\ C\sin(qd)e^{(d-x)p}, & x \ge d \end{cases} \tag{II.81}$$

Note that H_{0y} is tangential to the waveguide interfaces, and it is continuous at both $x = d$ and $x = -d$.

Since E_{0z} is also tangential to the waveguide interfaces, and it must be continuous at both $x = d$ and $x = -d$. Substituting (II.81) into (II.77) yields

$$E_{0z} = \frac{j}{\omega\varepsilon_0} \begin{cases} -\frac{p}{n_2^2} C\sin(qd)e^{p(d+x)}, & x \le -d \\ \frac{q}{n_1^2} C\cos(qx), & -d \le x \le d \\ -\frac{p}{n_2^2} C\sin(qd)e^{(d-x)p}, & x \ge d \end{cases} \tag{II.82}$$

At $x = \pm d$ we get

$$\frac{n_2^2}{n_1^2} qd \cot(qd) = -pd \tag{II.83}$$

II.4.F. Propagation Parameters

For TE modes, we have the ratio

$$\frac{E_{0y}}{H_{0x}} = -\frac{\omega\mu_0}{\beta} \tag{II.84}$$

A constant phase is satisfied whenever

$$\omega t - \beta z = \text{constant} \tag{II.85}$$

Differentiating with respect to time results in the following definition of the phase velocity

$$\frac{dz}{dt} = \frac{\omega}{\beta} = v_p \tag{II.86}$$

Using (II.28), we get

$$\frac{\omega}{\beta} = \frac{1}{\sqrt{\mu_0 \varepsilon}} \tag{II.87}$$

Therefore, we have

$$\beta = \omega \sqrt{\mu_0 \varepsilon} \tag{II.88}$$

Substituting (II.88) into (II.84) yields

$$\frac{E_{0y}}{H_{0x}} = -\sqrt{\frac{\mu_0}{\varepsilon}} \tag{II.89}$$

The negative sign in (II.89) indicates that $\vec{H}$ is directed in the negative x direction. The magnitude of the quantity in (II.89) in known as the medium intrinsic impedance;

$$\eta = \sqrt{\frac{\mu_0}{\varepsilon}} \tag{II.90}$$

For free space, we have

$$\begin{aligned} \eta_0 &= \sqrt{\frac{\mu_0}{\varepsilon_0}} \\ &\approx 377\ \Omega \end{aligned} \tag{II.91}$$

At the total phase of the field is equal to $\omega t - \beta z$, then for a fixed z the phase goes through a complete cycle of 2π radians in an interval (this interval is called the period)

$$T = \frac{2\pi}{\omega} \tag{II.92}$$

Similarly for a fixed t, the phase goes through a complete cycle of 2π radians in a distance (this distance is called the wavelength)

$$\lambda = \frac{2\pi}{\beta} \tag{II.93}$$

This is equivalent to

$$\beta = \frac{2\pi}{\lambda} \tag{II.94}$$

Note that using (II.86) we can write

$$\begin{aligned}\beta &= \frac{\omega}{v_p} \\ &= \frac{2\pi f}{v_p}\end{aligned} \tag{II.95}$$

Comparing (II.95) and (II.94) we have

$$\begin{aligned}\lambda &= \frac{v_p}{f} \\ &= \frac{c/f}{n} \\ &= \frac{\lambda_0}{n}\end{aligned} \tag{II.96}$$

The phase of the propagating wave can be expressed in the form

II.4.G. Group Velocity

The propagation constant in (II.94) is a function of frequency ω, and hence, the phase velocity in (II.86) is also a function of ω. Sometimes, the propagating signal can consist of more than one frequency (e.g., a modulated signal). Depending on the material, μ and ε can be functions of frequency as well. In such situations, the phase velocity is not enough to represent the velocity of propagation. A medium in which the velocity of propagation is a function of frequency is called a dispersive medium.

A modulated electromagnetic wave has sidebands. This means that the propagating wave consists of more than one frequency. When the carrier component and the sidebands propagate with different velocities, the relative phases of the carrier and the sideband change as the wave moves forward.

Consider an AM wave given at $z = 0$ by

$$e_{AM}(t) = E(1 + m\cos\omega_s t)\cos\omega_c t \tag{II.97}$$

This can be expanded as

$$e_{AM}(t) = E\cos\omega_c t + E\frac{m}{2}\left[\cos(\omega_c + \omega_s)t + \cos(\omega_c - \omega_s)t\right] \tag{II.98}$$

This can rewritten in the form

$$e_{AM}(t) = E\,\mathrm{Re}\left\{e^{j\omega_c t} + \frac{m}{2}\left[e^{j(\omega_c+\omega_s)t} + e^{j(\omega_c-\omega_s)t}\right]\right\} \tag{II.99}$$

The three frequency components ω_c, $\omega_c + \omega_s$ and $\omega_c - \omega_s$ have different values of the propagation constant β. Let's assume that the variation of β with ω is linear in the neighborhood of ω_c. Then, when ω changes by an amount $\Delta\omega$, β changes by an amount $\Delta\beta$ that is proportional to $\Delta\omega$. This can be expressed in the form

$$\Delta\beta = \Delta\omega \frac{d\beta}{d\omega} \tag{II.100}$$

The phase terms of the carrier and the upper and lower sideband components are thus given by

$$\gamma_c = \omega_c t - \beta_c z \tag{II.101}$$

$$\gamma_u = (\omega_c + \omega_s)t - \beta_u z \tag{II.102}$$

$$\gamma_l = (\omega_c - \omega_s)t - \beta_l z \tag{II.103}$$

where

$$\beta_u = \beta_c + \Delta\beta \tag{II.104}$$

$$\beta_l = \beta_c - \Delta\beta \tag{II.105}$$

After the wave in (II.99) propagates a distance z through this dispersive medium, it can be written as

$$e_{AM}(t,z) = E\,\mathrm{Re}\left\{e^{j(\omega_c t - \beta_c z)} + \frac{m}{2}\left[e^{j\left[(\omega_c+\omega_s)t-\beta_u z\right]} + e^{j\left[(\omega_c-\omega_s)t-\beta_l z\right]}\right]\right\} \tag{II.106}$$

Using (II.104) and (II.105) in (II.106) and applying the $\mathrm{Re}\{\cdot\}$ operation yields

$$e_{AM}(t) = E\left[1 + m\cos(\omega_s t - \Delta\beta z)\right]\cos(\omega_c t - \beta_c z) \tag{II.107}$$

$$\omega t - \beta z = \text{constant} \tag{II.108}$$

$$\frac{dz}{dt} = \frac{\omega}{\beta} = v_p \tag{II.109}$$

Note that in (II.107), the carrier component travels with the phase velocity $v_p = \omega_c / \beta_c$, while the sidebands travel with group velocity

$$\begin{aligned} v_g &= \frac{\omega_s}{\Delta\beta} \\ &= \frac{d\omega}{d\beta} \end{aligned} \quad \text{(II.110)}$$

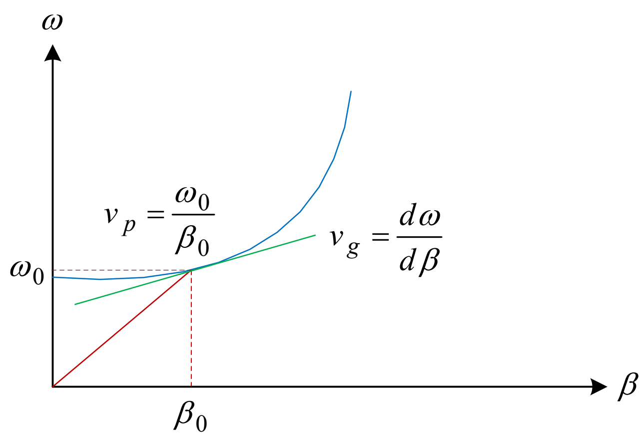

Figure II.17: Phase and group velocities

Example II.5

A plane wave with wavelength 1.3 µm travels in a medium with $\beta = 0.3(\omega - \omega_0)^{1/2}$, where $\omega_0 = 8.66 \times 10^6$ rad/s. Determine

a. the phase velocity
b. the group velocity
c. the medium refractive index

<u>***Solution***</u>

a. $\omega = 2\pi \frac{c}{\lambda} = 14.5 \times 10^{14}$ rad/s. $\beta = 0.3(\omega - \omega_0)^{1/2} = 7.25 \times 10^6$ rad/m. $v_p = \frac{\omega}{\beta} = 2 \times 10^8$ m/s.

b. $\omega = \frac{\beta^2}{0.09} + \omega_0$. $v_g = \frac{d\omega}{d\beta} = \frac{2}{0.09}\beta = 1.61 \times 10^8$ m/s.

c. $n = \frac{c}{v_p} = 1.5$.

II.4.H. Modal Dispersion in Planar Waveguide

Each TE and TM mode has its own propagation constant β. Hence, each mode has its own phase velocity $v_p(\beta)$ and its own group velocity $v_g(\beta)$. Propagation delays will be different. When several modes are received, several versions of the transmitted signal are received with different delays, resulting in signal spreading in time. This is referred to as modal (or intermodal) dispersion. Dispersion limits the maximum rate at which information can be transmitted through the system.

Note that qd cannot be larger than V. It can be seen from Figure II.14 that there can be only one mode in every $\pi/2$ on the qd scale. The number of supported modes is, therefore, governed by

$$M = \left\lceil \frac{2V}{\pi} \right\rceil \tag{II.111}$$

Modal dispersion is the difference between the longest and shortest mode propagation times. Signals propagate at the group velocity. Therefore, modal dispersion can be expressed as

$$\frac{\Delta\tau}{L} = \frac{1}{v_{g,\min}} - \frac{1}{v_{g,\max}} \tag{II.112}$$

The magnitude of this dispersion can be estimated by recognizing that β is that of the cladding material for modes that are close to cut-off (higher q), and is close to that of the core material for low-order modes (lower q). Note that for higher-order modes, most of the energy propagates in the cladding (decay in cladding is slow because of low p). For lower-order modes, most of the energy propagates in the core (decay in cladding is fast because of high p).

On the above basis, minimum and maximum values of the group velocities are those of the two materials. Therefore, we have

$$\frac{\Delta\tau}{L} = \frac{N_1}{c} - \frac{N_2}{c} \tag{II.113}$$

where

$$N = \frac{c}{v_g} \tag{II.114}$$

***

III. Step Index Optical Fiber

Step index optical fiber consists of two concentric cylinders, as shown in Figure III.1. The core has a radius a and a refractive index n_1. The cladding has a refractive index $n_2 < n_1$ and a much larger radius. The cladding is assumed to be infinitely extended in the radial direction.

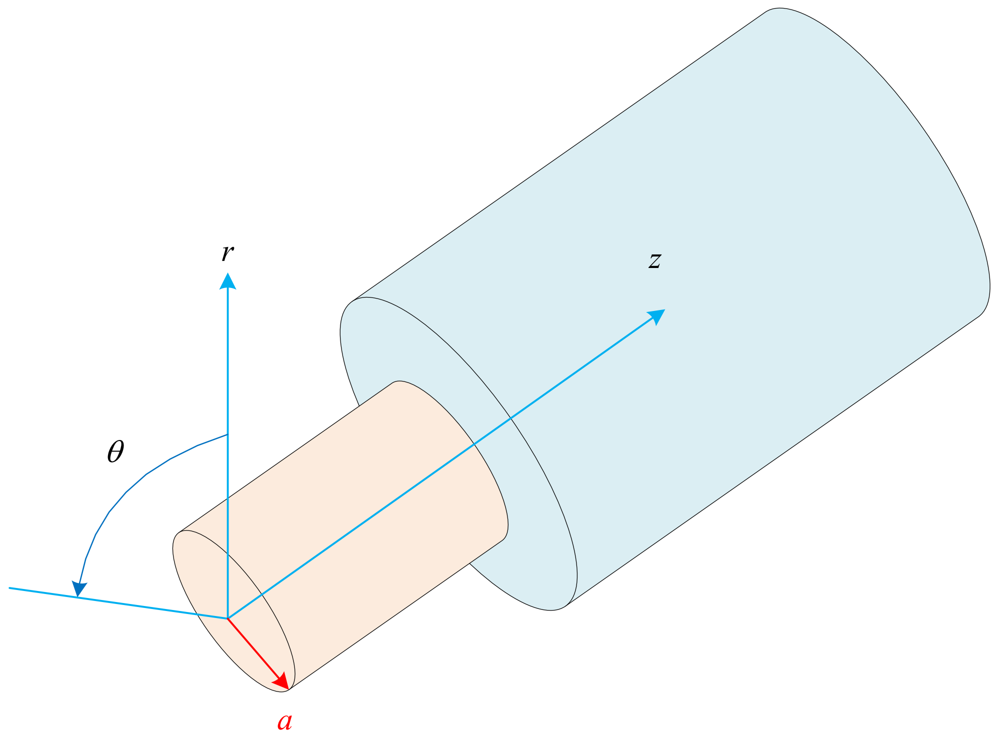

Figure III.1: Optical fiber in cylindrical coordinates

The refractive index profile is as shown in Figure III.2.

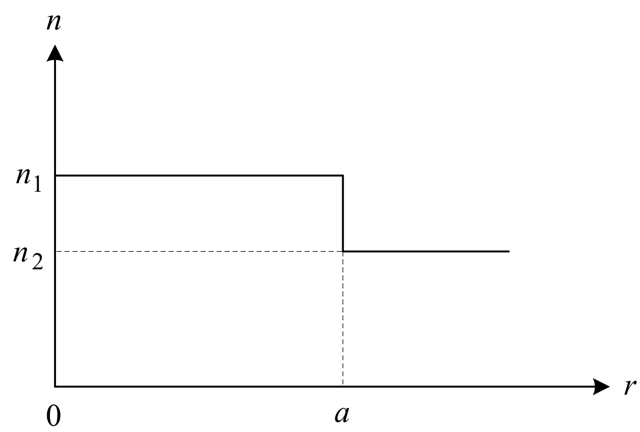

Figure III.2: Step index profile

III.1. Wave Equation and Boundary Conditions

$$\vec{\nabla}\times\vec{E}=-\mu\frac{\partial\vec{H}}{\partial t} \tag{III.1}$$

$$\vec{\nabla}\times\vec{H}=\varepsilon\frac{\partial\vec{E}}{\partial t} \tag{III.2}$$

Expanding the curl operators we get

$$\frac{1}{r}\frac{\partial E_z}{\partial\theta}-\frac{\partial E_\theta}{\partial z}=-\mu\frac{\partial H_r}{\partial t} \tag{III.3}$$

$$H_{0r}=\frac{j}{\omega\mu}\left(j\beta E_{0\theta}+\frac{1}{r}\frac{\partial E_{0z}}{\partial\theta}\right) \tag{III.4}$$

$$\frac{\partial E_r}{\partial z}-\frac{\partial E_z}{\partial r}=-\mu\frac{\partial H_\theta}{\partial t} \tag{III.5}$$

$$\frac{1}{r}\left(\frac{\partial(rE_\theta)}{\partial r}-\frac{\partial E_r}{\partial\theta}\right)=-\mu\frac{\partial H_z}{\partial t} \tag{III.6}$$

$$\frac{1}{r}\frac{\partial H_z}{\partial\theta}-\frac{\partial H_\theta}{\partial z}=\varepsilon\frac{\partial E_r}{\partial t} \tag{III.7}$$

$$\frac{\partial H_r}{\partial z}-\frac{\partial H_z}{\partial r}=\varepsilon\frac{\partial E_\theta}{\partial t} \tag{III.8}$$

$$E_{0\theta}=\frac{j}{\omega\varepsilon}\left(j\beta H_{0r}+\frac{\partial H_{0z}}{\partial r}\right) \tag{III.9}$$

$$\frac{1}{r}\left(\frac{\partial(rH_\theta)}{\partial r}-\frac{\partial H_r}{\partial\theta}\right)=\varepsilon\frac{\partial E_z}{\partial t} \tag{III.10}$$

Substituting (III.9) into (III.4) yields

$$H_{0r}=-\frac{j}{\kappa^2}\left(\beta\frac{\partial H_{0z}}{\partial r}-\omega\varepsilon\frac{1}{r}\frac{\partial E_{0z}}{\partial\theta}\right) \tag{III.11}$$

where

$$\begin{aligned}\kappa^2&=\omega^2\mu\varepsilon-\beta^2\\&=k^2-\beta^2\end{aligned} \tag{III.12}$$

Working similarly on (III.5)-(III.8) produces

$$H_{0\theta}=-\frac{j}{\kappa^2}\left(\beta\frac{1}{r}\frac{\partial H_{0z}}{\partial\theta}+\omega\varepsilon\frac{\partial E_{0z}}{\partial r}\right) \tag{III.13}$$

$$E_{0r}=-\frac{j}{\kappa^2}\left(\beta\frac{\partial E_{0z}}{\partial r}+\omega\mu\frac{1}{r}\frac{\partial H_{0z}}{\partial\theta}\right) \tag{III.14}$$

$$E_{0\theta}=-\frac{j}{\kappa^2}\left(\beta\frac{1}{r}\frac{\partial E_{0z}}{\partial\theta}-\omega\mu\frac{\partial H_{0z}}{\partial r}\right) \tag{III.15}$$

Note that the four field components in the r and θ have been expresses in terms of the two field components E_{0z} and H_{0z}. Next, we determine E_{0z} and H_{0z}.

The wave equation for E_{0z} is given by

$$\nabla^2E_{0z}+\omega^2\mu\varepsilon E_{0z}=0 \tag{III.16}$$

Using the definition of the Laplacian operator in cylindrical coordinates,

$$\frac{\partial^2}{\partial r^2}E_{0z}+\frac{1}{r}\frac{\partial}{\partial r}E_{0z}+\frac{1}{r^2}\frac{\partial^2}{\partial\theta^2}E_{0z}+\frac{\partial^2}{\partial z^2}E_{0z}+\omega^2\mu\varepsilon E_{0z}=0 \tag{III.17}$$

Substituting $\partial/\partial z=-j\beta$ ($\partial^2/\partial z^2=-\beta^2$) in (III.17) gives

$$\frac{\partial^2}{\partial r^2}E_{0z}+\frac{1}{r}\frac{\partial}{\partial r}E_{0z}+\frac{1}{r^2}\frac{\partial^2}{\partial\theta^2}E_{0z}+\kappa^2E_{0z}=0 \tag{III.18}$$

Similarly, the wave equation for H_{0z} is given by

$$\frac{\partial^2}{\partial r^2}H_{0z}+\frac{1}{r}\frac{\partial}{\partial r}H_{0z}+\frac{1}{r^2}\frac{\partial^2}{\partial \theta^2}H_{0z}+\kappa^2 H_{0z}=0 \tag{III.19}$$

Assume

$$E_{0z}=Ag(r)h(\theta) \tag{III.20}$$

The function $h(\theta)$ must be periodic in θ with period $2\pi/\nu$, where ν is an integer called the azimuthal index. Let

$$h(\theta)=e^{j\nu\theta} \tag{III.21}$$

$$\frac{d^2}{dr^2}g(r)+\frac{1}{r}\frac{d}{dr}g(r)+\left(\kappa^2-\frac{\nu^2}{r^2}\right)g(r)=0 \tag{III.22}$$

This a Bessel differential equation, the solutions of which are Bessel functions. The solutions of (III.22) must be finite for $r \le a$ (core), and must approach zero for $r >> a$ (cladding). Bessel function of the first kind $J_\nu(\kappa r)$ (generally oscillatory) can be used in the core, while modified Bessel function of the second kind $K_\nu(\gamma r)$ can be used in the cladding. Hence, the following forms of solution will be adopted:

$$g(r)=\begin{cases} J_\nu(\kappa r), & r \le a \\ K_\nu(\gamma r), & r > a \end{cases} \tag{III.23}$$

where

$$\kappa^2 = n_1^2 k^2 - \beta^2 \tag{III.24}$$

$$\gamma^2 = \beta^2 - n_2^2 k^2 \tag{III.25}$$

Graphs of $J_\nu(x)$ are shown in Figure III.3 for $\nu = 0,1,2,3$. Graphs of $K_\nu(x)$ are shown in Figure III.4 for $\nu = 0,1,2,3$. Note that $K_\nu(x) > 0$ for all values of ν and x, and that $K_\nu(0) > 0$ for all values of ν.

Eliminating β in (III.24) and (III.25), we get

$$\kappa^2+\gamma^2=(n_1^2-n_2^2)k^2 \tag{III.26}$$

Let's define the normalized frequency as

$$V=\frac{2\pi}{\lambda}a\sqrt{n_1^2-n_2^2} \tag{III.27}$$

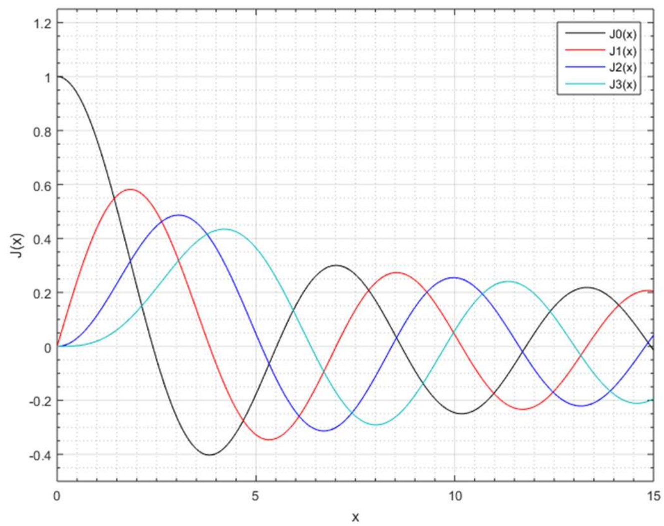

Figure III.3: Bessel functions of the first kind

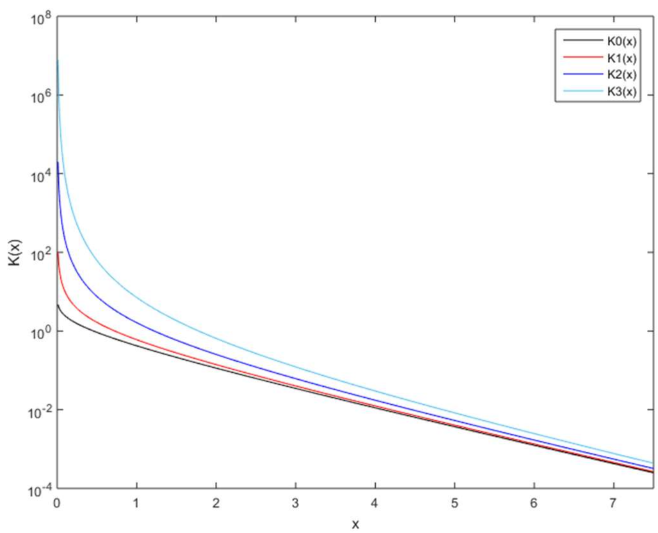

Figure III.4: Modified Bessel functions of the second kind

Then, we obviously have

$$(\kappa a)^2 + (\gamma a)^2 = V^2 \tag{III.28}$$

Note that tangential field components are those in the z and θ, and that these components must be continuous around $r = a$. Applying these boundary conditions leads to the eigenvalue equations. Deriving the eigenvalue equations requires determining a fourth-order determinant. Generally, this is mathematically difficult, but is not of practical interest in most cases.

The case that represents most optical fibers, especially those with better transmission characteristics is that for which $n_1 - n_2$ compared to n_1 or n_2 is small. Fibers with such a condition satisfied are known as weakly guiding fibers.

III.2. Weakly Guiding Fibers

The restriction $n_1 - n_2 << n_2$ leads to desirable properties of the optical fiber. Optical fibers that satisfy this constraint are called weakly guiding fibers. One of the advantages of imposing this restriction is the simplification of the eigenvalue equations. The resulting equation is

$$\frac{J_\nu(\kappa a)}{J_{\nu-1}(\kappa a)} = -\frac{\kappa}{\gamma}\frac{K_\nu(\gamma a)}{K_{\nu-1}(\gamma a)} \tag{III.29}$$

For the particular case of $\nu = 0$, we have

$$\frac{J_0(\kappa a)}{J_{-1}(\kappa a)} = -\frac{\kappa}{\gamma}\frac{K_0(\gamma a)}{K_{-1}(\gamma a)} \tag{III.30}$$

Consider the Bessel function identities

$$J_{-1}(\kappa a) = -J_1(\kappa a) \tag{III.31}$$

The identity in (III.31) for all odd value of ν in $J_\nu(\kappa a)$. For even ν, the identity becomes $J_{-\nu}(\kappa a) = J_\nu(\kappa a)$.

$$K_{-1}(\kappa a) = K_1(\kappa a) \tag{III.32}$$

Using (III.31) and (III.32) in (III.30) yields

$$\frac{J_1(\kappa a)}{J_0(\kappa a)} = \frac{\gamma}{\kappa}\frac{K_1(\gamma a)}{K_0(\gamma a)} \tag{III.33}$$

Equation (III.33) can be solved using the graphical technique, similar to the way of solving the eigenvalue equation of the planar waveguide. Note that we can rewrite (III.33) in the form

$$\kappa a\frac{J_1(\kappa a)}{J_0(\kappa a)} - \gamma a\frac{K_1(\gamma a)}{K_0(\gamma a)} = 0 \tag{III.34}$$

Using (III.28), solving (III.34) is equivalent to finding the roots of

$$g_0(\kappa a) = \kappa a\frac{J_1(\kappa a)}{J_0(\kappa a)} - \sqrt{V^2 - (\kappa a)^2}\,\frac{K_1\left(\sqrt{V^2-(\kappa a)^2}\right)}{K_0\left(\sqrt{V^2-(\kappa a)^2}\right)} \tag{III.35}$$

This equation can be sketched for different values of κa. The points where $g_0(\kappa a)$ is zero represent the allowed values of κa. The corresponding values of γa can be found from (III.28).

Example III.1

Suppose $V = 8$. Equation (III.35) is sketched below for $\nu = 0$.

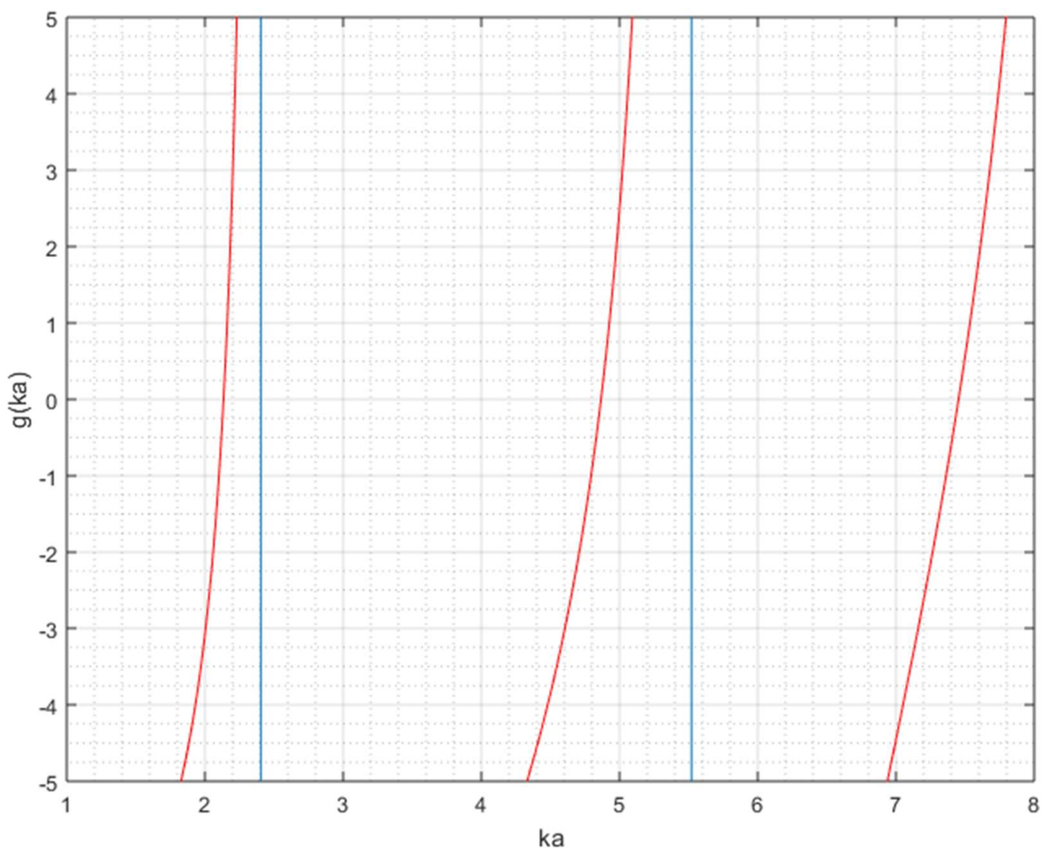

Solutions: $\kappa a = 2.1346,\ 4.8658,\ 7.4528$. Therefore, $\gamma a = 7.7100,\ 6.3501,\ 2.9079$.

For $\nu = 1$, the eigenvalue equation in (III.29) becomes

$$\frac{J_1(\kappa a)}{J_0(\kappa a)} = -\frac{\kappa}{\gamma}\frac{K_1(\gamma a)}{K_0(\gamma a)} \tag{III.36}$$

This can also be solved using the graphical technique. Note that we can rewrite (III.36) in the form

$$\gamma\frac{J_1(\kappa a)}{J_0(\kappa a)} + \kappa\frac{K_1(\gamma a)}{K_0(\gamma a)} = 0 \tag{III.37}$$

Using (III.28), solving (III.37) is equivalent to finding the roots of

$$g_1(\kappa a) = \sqrt{V^2 - (\kappa a)^2}\,\frac{J_1(\kappa a)}{J_0(\kappa a)} + \kappa a \frac{K_1\left(\sqrt{V^2 - (\kappa a)^2}\right)}{K_0\left(\sqrt{V^2 - (\kappa a)^2}\right)} \tag{III.38}$$

This equation can be sketched for different values of κa. The points $g_1(\kappa a)$ is zero represent the allowed values of κa. The corresponding values of γa can be found from (III.28).

Example III.2

Suppose $V = 8$. Equation (III.38) is sketched below for $\nu = 1$.

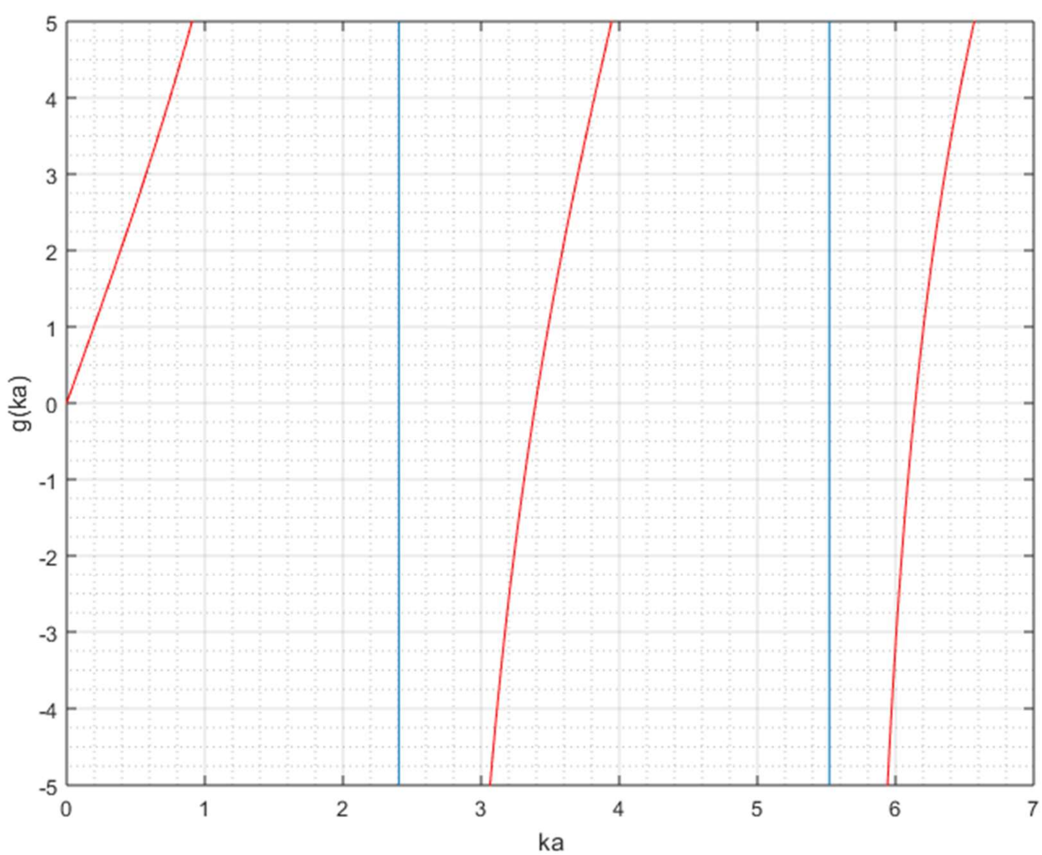

Solutions: $\kappa a = 3.3942,\ 6.1425$. Therefore, $\gamma a = 7.2443,\ 5.1254$.

For $\nu > 1$, the right side of (III.29) becomes always negative. As ν increases, the first infinite discontinuity of $J_\nu(\kappa a)/J_{\nu-1}(\kappa a)$ moves to the right. At some value ν_c, the first infinite discontinuity of $J_{\nu_c}(\kappa a)/J_{\nu_c-1}(\kappa a)$ exceeds V, meaning that the eigenvalue equation has no solutions. Note that the following condition is satisfied by the highest order propagating mode.

$$J_{\nu_c-1}(\kappa a) = 0 \tag{III.39}$$

III.2.A. Zeros of Bessel Functions

Table III.1: Zeros of $J_\nu(\kappa a)/J_{\nu-1}(\kappa a)$

$J_0(x)$	$J_1(x)$	$J_2(x)$	$J_3(x)$	$J_4(x)$	$J_5(x)$
2.405	3.832	5.136	6.380	7.588	8.772
5.520	7.016	8.417	9.761	11.065	12.339
8.634	10.173	11.620	13.015	14.372	15.700
11.792	13.324	14.796	16.223	17.616	18.980
14.931	16.471	17.960	19.409	20.827	22.218
18.071	19.616	21.117	22.583		
21.212	22.760				

Example III.3

Suppose $V = 8$.

1. For $\nu = 4$, the first zero crossing of $J_\nu(\kappa a)/J_{\nu-1}(\kappa a) = J_4(\kappa a)/J_3(\kappa a)$ is at $\kappa a = 7.588$. This value is smaller than V. This means that a mode exists for $\nu = 4$. All other zero crossings of $J_4(\kappa a)/J_3(\kappa a)$ take place for $\kappa a > V$, meaning that only one mode for $\nu = 4$ exists.
2. For $\nu > 4$, the first zero crossings of $J_\nu(\kappa a)/J_{\nu-1}(\kappa a)$ are all larger than V, meaning no modes for $\nu > 4$ exist.

Example III.4

Suppose $V = 8$. Equation (III.29) is sketched below for $\nu = 2$.

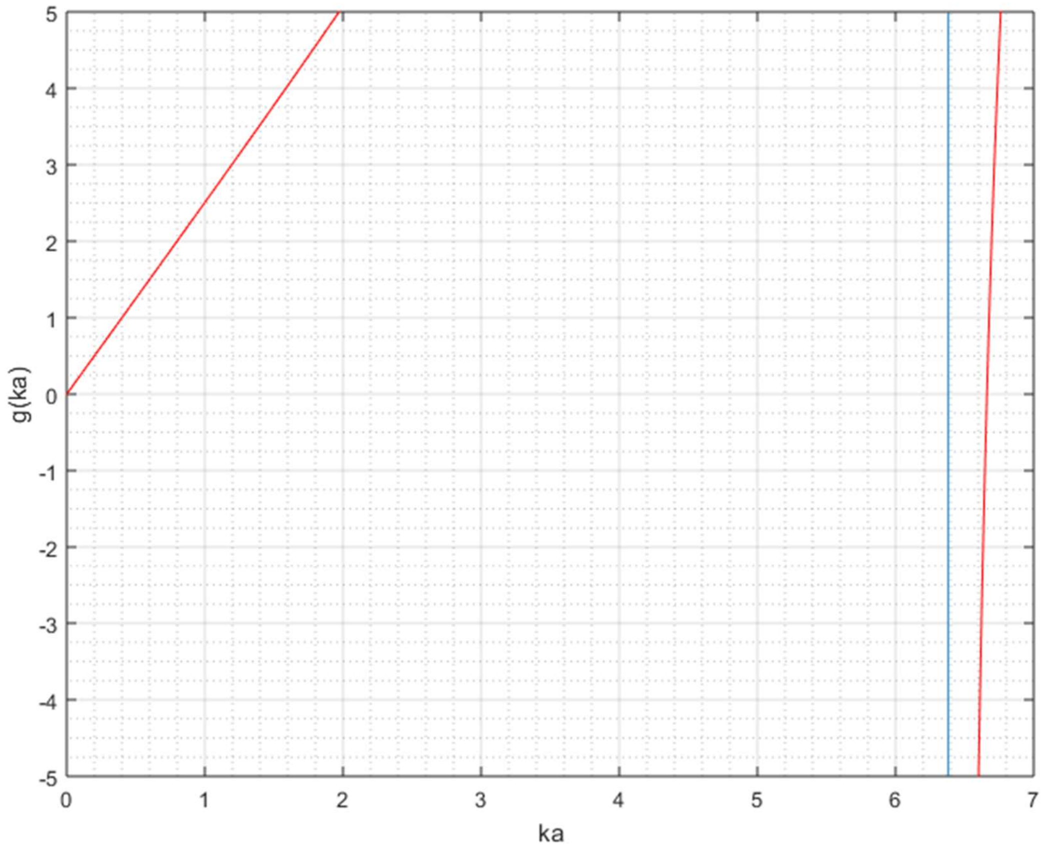

Solutions: $\kappa a = 6.6615$. Therefore, $\gamma a = 4.4299$.

***

IV. Transmission Characteristics of Optical Fibers

IV.1. Introduction

The huge potential bandwidth of optical communications helped stimulate the birth of the idea that a dielectric waveguide made of glass could be used to carry wideband telecommunication signals. The transmission characteristics are of utmost importance when the suitability of optical fibers for communication purposes is investigated. The transmission characteristics of most interest are those of attenuation (or loss) and dispersion. In principle, attenuation affects the communication link length, while dispersion limits the achievable transmission rate. There are other transmission characteristics of fibers, like modal noise and nonlinear effects.

IV.2. Attenuation

The attenuation or transmission loss of optical fibers has proved to be one of the most important factors in bringing about their wide acceptance in telecommunications. As channel attenuation largely determined the maximum transmission distance prior to signal restoration, optical fiber communications became especially attractive when the transmission losses of fibers were reduced below those of the competing metallic conductors (less than 5 dB/km).

In optical fiber communications the attenuation is usually expressed in dB per unit length (i.e. dB/km). Mathematically, the signal attenuation per unit length α_{dB} can be expressed as

$$\alpha_{\text{dB}} = \frac{10\log_{10}\left(\frac{P_i}{P_o}\right)}{L} \tag{IV.1}$$

where P_i is the fiber input power, P_o is the fiber output power, and L is the fiber link length. α_{dB} is sometimes referred to as the fiber loss parameter.

Example IV.1

The mean optical power launched into an 8 km length of fiber is 120 μW. The mean optical power at the fiber output is 3 μW. Determine

a the overall signal attenuation or loss in dB through the fiber assuming there are no connectors or splices,
b the signal attenuation per kilometer for the fiber,
c the overall signal attenuation for a 10 km optical link using the same fiber with splices at 1 km intervals, each giving an attenuation of 1 dB,
d the numerical input/output power ratio in ***c***.

Solution

a Attenuation $= 10\log_{10}\left(\frac{P_i}{P_o}\right) = 10\log_{10}\left(\frac{120}{3}\right) = 10\log_{10} 40 = 16 \text{ dB}$

b $\alpha_{\text{dB}} = \frac{16}{8} = 2 \text{ dB/km}$

c Losses are due to fiber and to slices:

Fiber Loss: $\alpha_{\text{dB}} L = 2(10) = 20 \text{ dB}$

Splice Loss = 1(9) = 9 dB

Total Loss = 20 + 9 = 29 dB

d $\frac{P_i}{P_o} = 10^{2.9} = 794.28$

A number of mechanisms are responsible for the signal attenuation within optical fibers. These mechanisms are influenced by the material composition, the preparation and purification technique, and the waveguide structure. They may be categorized within several major areas which include material absorption, material scattering (linear and nonlinear scattering), curve and microbending losses, mode coupling radiation losses and losses due to leaky modes. There are also losses at connectors and splices.

IV.2.A. MATERIAL ABSORPTION LOSSES IN SILICA GLASS FIBERS

Intrinsic Absorption

An absolutely pure silicate glass has little intrinsic absorption due to its basic material structure in the near-infrared region. Any material absorbs at certain wavelengths corresponding to the electronic and vibrational resonances associated with specific molecules. For silica (SiO_2) molecules, electronic resonances occur in the ultraviolet region ($\lambda < 0.4$ μm), whereas vibrational resonances occur in the infrared region ($\lambda > 0.78$ μm). Because of the amorphous nature of fused silica, these resonances are in the form of absorption bands whose tails extend into the visible region.

Intrinsic material absorption for silica in the wavelength range 0.8–1.6 μm is below 0.1 dB/km. In fact, it is less than 0.03 dB/km in the 1.3–1.6 μm region that is commonly used for lightwave communications.

Extrinsic Absorption

Extrinsic absorption results from the presence of impurities. Transition-metal impurities such as Fe, Cu, Co, Ni, Mn, and Cr absorb strongly in the wavelength range 0.6–1.6μm. Their amount should be reduced to below 1 part per billion to obtain a loss level below 1 dB/km. Such high-purity silica can be obtained by using modern techniques. The main source of extrinsic absorption in state-of-the-art silica fibers is the presence of water vapors. A vibrational resonance of the OH ion occurs near 2.73 μm. Its harmonic and combination tones with silica produce absorption at the 1.39-, 1.24-, and 0.95-μm wavelengths. Even a concentration of 1 part per million can cause a loss of about 50 dB/km at 1.39 μm. The OH ion concentration is reduced to below 10^{-8} in modern fibers to lower the 1.39-μm peak below 1 dB/km. In a new kind of fiber, known as the dry fiber, the OH ion concentration is reduced to such low levels that the 1.39-μm peak almost disappears. Such fibers can be used to transmit WDM signals over the entire 1.3–1.6 μm wavelength range.

IV.2.B. LINEAR SCATTERING LOSSES

Linear scattering mechanisms cause the transfer of some or all of the optical power contained within one propagating mode to be transferred linearly (proportionally to the mode power) into a different mode. This process tends to result in attenuation of the transmitted light as the transfer may be to a leaky or radiation mode which does not continue to propagate within the fiber core, but is radiated from the fiber. It must be noted that as with all linear processes, there is no change of frequency on scattering.

Linear scattering may be categorized into two major types: Rayleigh and Mie scattering. Both result from the nonideal physical properties of the manufactured fiber.

Rayleigh Scattering

Rayleigh scattering results from inhomogeneities of a random nature occurring on a small scale compared with the wavelength of the light. These inhomogeneities manifest themselves as refractive index fluctuations and arise from density and compositional variations which are frozen into the glass lattice on cooling. The subsequent scattering due to the density fluctuations, which is in almost all directions, produces an attenuation proportional to $1/\lambda^4$.

Mie Scattering

Mie scattering occurs at inhomogeneities which are comparable in size with the guided wavelength. These result from the nonperfect cylindrical structure of the waveguide and may be caused by fiber imperfections such as irregularities in the core–cladding interface, core–cladding refractive index differences along the fiber length, diameter fluctuations, strains and bubbles. When the scattering inhomogeneity size is greater than $\lambda/10$, the scattered intensity which has an angular dependence can be very large.

IV.2.C. NONLINEAR SCATTERING LOSSES

Optical waveguides do not always behave as completely linear channels whose increase in output optical power is directly proportional to the input optical power. Several nonlinear effects occur, which in the case of scattering cause disproportionate attenuation, usually at high optical power levels. This nonlinear scattering causes the optical power from one mode to be transferred in either the forward or backward direction to the same, or other modes, at a different frequency. It depends critically upon the optical power density within the fiber and hence only becomes significant above threshold power levels.

The most important types of nonlinear scattering within optical fibers are stimulated Brillouin and Raman scattering, both of which are usually only observed at high optical power densities in long single-mode fibers. These scattering mechanisms in fact give optical gain but with a shift in frequency, thus contributing to attenuation for light transmission at a specific wavelength.

However, it may be noted that such nonlinear phenomena can also be used to give optical amplification in the context of integrated optical techniques.

Stimulated Brillouin Scattering

Stimulated Brillouin scattering (SBS) may be regarded as the modulation of light through thermal molecular vibrations within the fiber. The scattered light appears as upper and lower sidebands which are separated from the incident light by the modulation frequency. The incident photon in this scattering process produces a phonon[2] of acoustic frequency as well as a scattered photon. This produces an optical frequency shift which varies with the scattering angle because the frequency of the sound wave varies with acoustic wavelength. The frequency shift is a maximum in the backward direction, reducing to zero in the forward direction, making SBS a mainly backward process.

Brillouin scattering is only significant above a threshold power density. Threshold power in Watts is given by

$$P_B = 4.4 \times 10^{-3} d^2 \lambda^2 \alpha_{\text{dB}} \nu \qquad \text{(IV.2)}$$

where d is the fiber core diameter in μm, λ is the operating wavelength in μm, α_{dB} is the fiber loss in dB/km, and ν is the source bandwidth in GHz. Note that (IV.2) allows the determination of the threshold optical power which must be launched into a single-mode optical fiber before SBS occurs.

Stimulated Raman Scattering

Stimulated Raman scattering (SRS) is similar to SBS except that a high-frequency optical phonon rather than an acoustic phonon is generated in the scattering process. Also, SRS can occur in both the forward and backward directions in an optical fiber, and may have an optical power threshold of up to three orders of magnitude higher than the Brillouin threshold in a particular fiber.

Threshold optical power for SRS in a long single-mode fiber is given by

$$P_R = 5.9 \times 10^{-2} d^2 \lambda \alpha_{\text{dB}} \qquad \text{(IV.3)}$$

Example IV.2

A long single-mode optical fiber has an attenuation of 0.5 dB/km when operating at a wavelength of 1.3 μm. The fiber core diameter is 6 μm and the laser source bandwidth is 600 MHz. Compare the threshold optical powers for stimulated Brillouin and Raman scattering within the fiber at the wavelength specified.

Solution

[2] The phonon is a quantum of an elastic wave in a crystal lattice. When the elastic wave has a frequency f, the quantized unit of the phonon has energy hf joules, where h is Planck's constant.

$$\begin{aligned} P_B &= 4.4 \times 10^{-3} \times 6^2 \times 1.3^2 \times 0.5 \times 0.6 \\ &= 80.3 \text{ mW} \end{aligned}$$

$$\begin{aligned} P_R &= 5.9 \times 10^{-2} \times 6^2 \times 1.3 \times 0.5 \\ &= 1.38 \text{ W} \end{aligned}$$

In Example IV.2, the Brillouin threshold occurs at an optical power level of around 80 mW while the Raman threshold is approximately 17 times larger. It is therefore apparent that the losses introduced by nonlinear scattering may be avoided by use of a suitable optical signal level (i.e. working below the threshold optical powers). However, it must be noted that the Brillouin threshold has been reported as occurring at optical powers as low as 10 mW in single-mode fibers. Nevertheless, this is still a high power level for optical communications and may be easily avoided. SBS and SRS are not usually observed in multimode fibers because their relatively large core diameters make the threshold optical power levels extremely high. Moreover, it should be noted that the threshold optical powers for both these scattering mechanisms may be increased by suitable adjustment of the other parameters in (IV.2) and (IV.3). In this context, operation at the longest possible wavelength is advantageous although this may be offset by the reduced fiber attenuation (from Rayleigh scattering and material absorption) normally obtained.

IV.3. Dispersion

Dispersion of the transmitted optical signal causes distortion for both digital and analog transmission along optical fibers. When considering the major implementation of optical fiber transmission which involves some form of digital modulation, then dispersion mechanisms within the fiber cause broadening of the transmitted light pulses as they travel along the channel. An example signal at the beginning of a fiber link is shown in Figure IV.1.

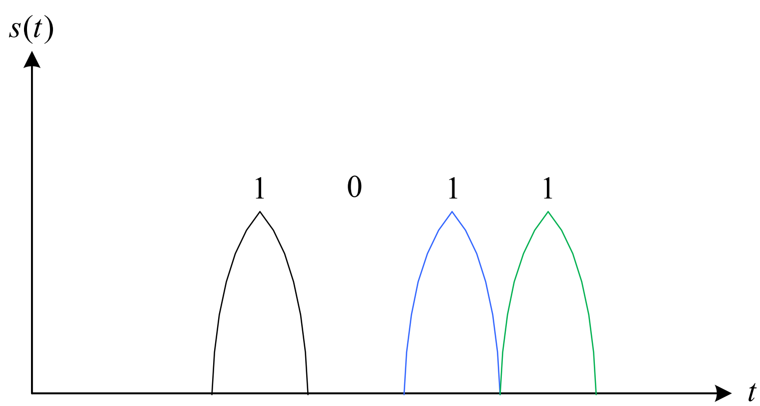

Figure IV.1: Signal at $z = 0$

After traveling to $z = L_1$, the signal is shown in Figure IV.2, where it can be observed that each pulse broadens and overlaps with its neighbors.

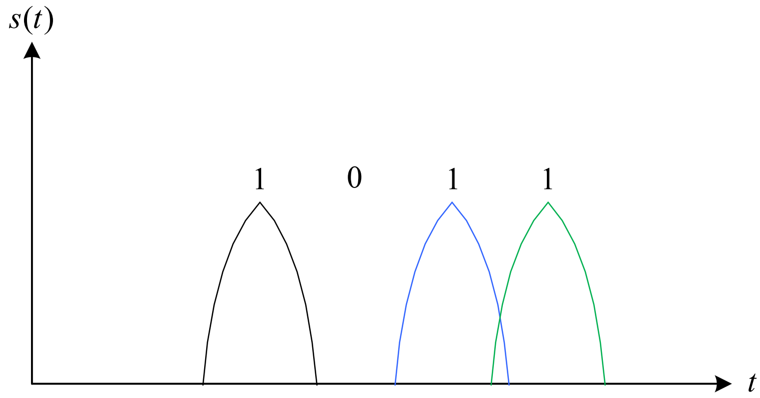

Figure IV.2: Signal at $z = L_1$

The pulses become almost indistinguishable after traveling to $z = L_2 > L_1$, as shown in Figure IV.3.

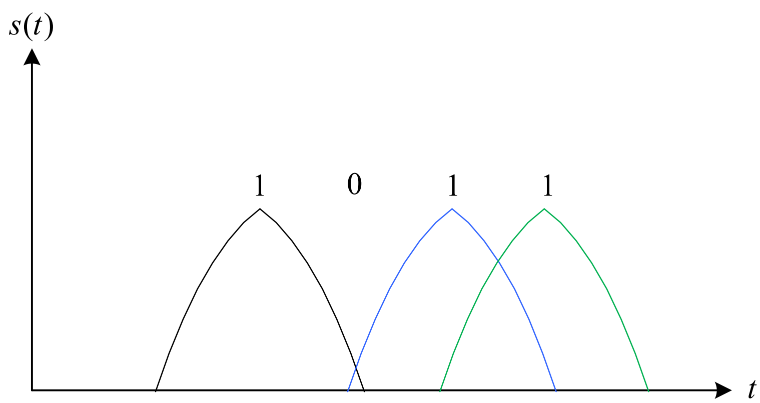

Figure IV.3: Signal at $z = L_2 > L_1$

The above effect is known as intersymbol interference (ISI). Thus an increasing number of errors may be encountered on the digital optical channel as the ISI becomes more pronounced. The error rate is also a function of the signal attenuation on the link and the subsequent signal-to-noise ratio (SNR) at the receiver. Signal dispersion limits the maximum possible bandwidth attainable with a particular optical fiber to the point where individual symbols can no longer be distinguished.

A conservative estimate of the maximum possible link bit rate is given by

$$B_T = \frac{1}{2\tau} \tag{IV.4}$$

where it has been assumed that the pulse width is equal to τ, and that the pulse broadening due to dispersion is also equal to τ. Another more accurate estimate of the maximum bit rate for an optical channel with dispersion may be obtained by considering the light pulses at the input to have a Gaussian shape with an rms width of σ. The maximum bit rate is given approximately by

$$B_T \leq \frac{0.2}{\sigma} \tag{IV.5}$$

Equation (IV.5) gives a reasonably good approximation for other pulse shapes which may occur on the channel resulting from the various dispersive mechanisms within the fiber.

The conversion of bit rate to bandwidth in hertz depends on the digital coding format used. When a nonreturn-to-zero code is employed, the binary "1" level is held for the whole bit period τ. In this case

$$B_T = 2B \tag{IV.6}$$

However, when a return-to-zero code is considered, the binary "1" level is held for only part (usually half) of the bit period, i.e., $\tau/2$. In this case

$$B_T = B \tag{IV.7}$$

IV.4. Chromatic Dispersion

Chromatic or intramodal dispersion may occur in all types of optical fiber and results from the finite spectral linewidth of the optical source. Since optical sources do not emit just a single frequency but a band of frequencies (in the case of the injection laser corresponding to only a fraction of a percent of the center frequency, whereas for the LED it is likely to be a significant percentage), then there may be propagation delay differences between the different spectral components of the transmitted signal. This causes broadening of each transmitted mode and hence intramodal dispersion. The delay differences may be caused by the dispersive properties of the waveguide material (material dispersion) and also guidance effects within the fiber structure (waveguide dispersion).

IV.4.A. Material Dispersion

Pulse broadening due to material dispersion results from the different group velocities of the various spectral components launched into the fiber from the optical source. It occurs when the phase velocity of a plane wave propagating in the dielectric medium varies nonlinearly with wavelength, and a material is said to exhibit material dispersion when the second differential of the refractive index with respect to wavelength is not zero (i.e. $d^2n/d\lambda^2 \neq 0$).

Let's consider the group velocity in the fiber

$$\begin{aligned} v_g &= \frac{d\omega}{d\beta} \\ &= \frac{d\lambda}{d\beta}\frac{d\omega}{d\lambda} \end{aligned} \tag{IV.8}$$

This can be shown to be equal to

$$\begin{aligned} v_g &= \frac{c}{n_1 - \lambda \frac{dn_1}{d\lambda}} \\ &= \frac{c}{N_g} \end{aligned} \qquad \text{(IV.9)}$$

where

$$N_g = n_1 - \lambda \frac{dn_1}{d\lambda} \qquad \text{(IV.10)}$$

Therefore,

$$\begin{aligned} \tau_g &= \frac{1}{v_g} \\ &= \frac{1}{c}\left(n_1 - \lambda \frac{dn_1}{d\lambda}\right) \end{aligned} \qquad \text{(IV.11)}$$

IV.4.B. WAVEGUIDE DISPERSION

IV.5. Nonlinear Effects

***

V. Laser Light Sources

V.1.A. Basic Concepts

The optical source is often considered to be the active component in an optical fiber communication system. Its fundamental function is to convert electrical energy in the form of a current into optical energy (light) in an efficient manner which allows the light output to be effectively launched or coupled into the optical fiber.

To gain an understanding of the light-generating mechanisms within the major optical sources used in optical fiber communications it is necessary to consider both the fundamental atomic concepts and the device structure. In this context the requirements for the laser source are far more stringent than those for the LED. Unlike the LED, strictly speaking, the laser is a device which amplifies light – hence the derivation of the term LASER as an acronym for **Light Amplification by Stimulated Emission of Radiation**. Lasers, however, are seldom used as amplifiers since there are practical difficulties in relation to the achievement of high gain while avoiding oscillation from the required energy feedback. Thus the practical realization of the laser is as an optical oscillator. The operation of the device may be described by the formation of an electromagnetic standing wave within a cavity (or optical resonator) which provides an output of monochromatic, highly coherent radiation. By contrast the LED provides optical emission without an inherent gain mechanism. This results in incoherent light output.

V.1.B. Absorption and Emission of Radiation

The interaction of light with matter takes place in discrete packets of energy or quanta, called photons. Furthermore, the quantum theory suggests that atoms exist only in certain discrete energy states such that absorption and emission of light causes them to make a transition from one discrete energy state to another. The frequency of the absorbed or emitted radiation f is related to the difference in energy E between the higher energy state E_2 and the lower energy state E_1 by the expression

$$\begin{aligned} E &= E_2 - E_1 \\ &= hf \end{aligned} \tag{V.1}$$

where $h = 6.626 \times 10^{-34}$ J.s is Planck's constant.

A single electron transition between two energy levels within the atom will provide a change in energy suitable for the absorption or emission of a photon. It must be noted, however, that modern quantum theory gives a probabilistic description which specifies the energy levels in which electrons are most likely to be found.

Figure V.1 illustrates a two energy state or level atomic system where an atom is initially in the lower energy state E_1. When a photon with energy $E_2 - E_1$ is incident on the atom it may be excited into the higher energy state E_2 through absorption of the photon. This process is referred to as stimulated absorption.

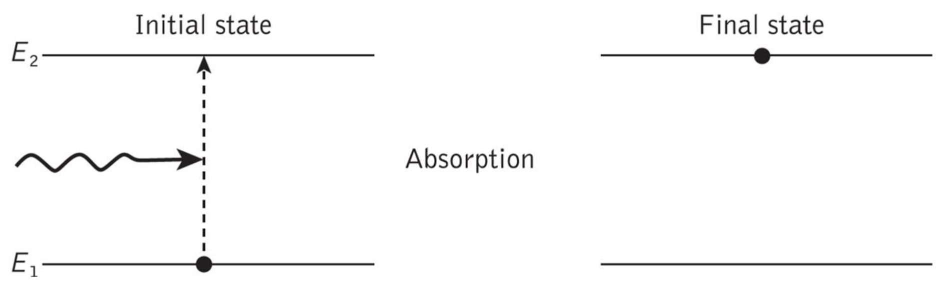

Figure V.1: Absorption

Alternatively, when the atom is initially in the higher energy state E_2 it can make a transition to the lower energy state E_1 providing the emission of a photon at a frequency corresponding to (V.1). This emission process can occur by spontaneous emission in which the atom returns to the lower energy state in an entirely random manner. Spontaneous emission is shown in Figure V.2. The random nature of the spontaneous emission process where light is emitted by electronic transitions from a large number of atoms gives incoherent radiation. A similar emission process in semiconductors provides the basic mechanism for light generation within the LED.

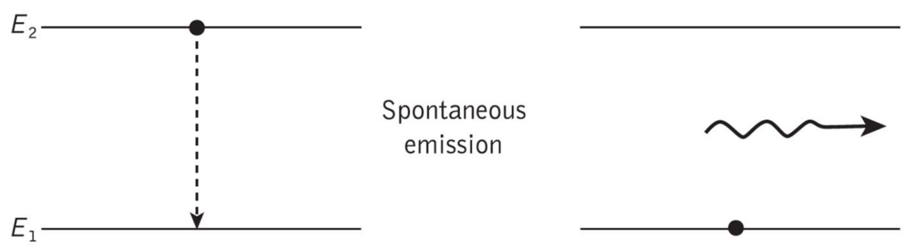

Figure V.2: Spontaneous emission

The photon emission process can also occur by stimulated emission when a photon having an energy equal to the energy difference between the two states $E_2 - E_1$ interacts with the atom in the upper energy state causing it to return to the lower state with the creation of a second photon. Stimulated emission is shown in Figure V.3.

It is the stimulated emission process, however, which gives the laser its special properties as an optical source. Firstly, the photon produced by stimulated emission is generally of an identical energy[3] to the one which caused it and hence the light associated with them is of the same frequency. Secondly, the light associated with the stimulating and stimulated photon is in phase and has the same polarization. Therefore, in contrast to spontaneous emission, coherent radiation is obtained. Furthermore, this means that when an atom is stimulated to emit light energy by an incident wave, the liberated energy can add to the wave in a constructive manner, providing amplification.

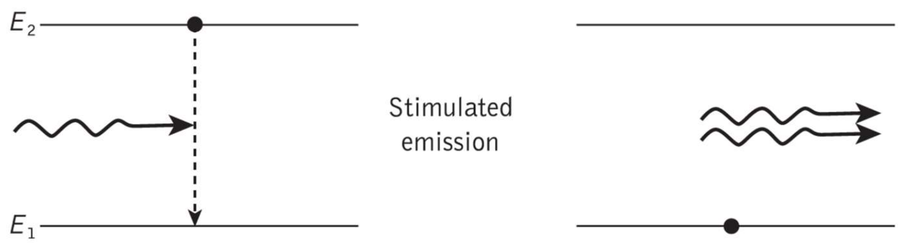

Figure V.3: Stimulated emission

Under the conditions of thermal equilibrium the lower energy level E_1 of the two-level atomic system contains more atoms than the upper energy level E_2. This situation is normal for structures at room temperature. However, to achieve optical amplification it is necessary to create a nonequilibrium distribution of atoms such that the population of the upper energy level is greater than that of the lower energy level (i.e. $N_2 > N_1$). This condition is known as population inversion. In order to achieve population inversion it is necessary to excite atoms into the upper energy level E_2 and hence obtain a nonequilibrium distribution. This process is achieved using an external energy source and is referred to as 'pumping'.

V.1.C. Optical Feedback and Laser Oscillation

Light amplification in the laser occurs when a photon colliding with an atom in the excited energy state causes the stimulated emission of a second photon and then both these photons release two more. Continuation of this process effectively creates avalanche multiplication, and when the electromagnetic waves associated with these photons are in phase, amplified coherent emission is obtained. To achieve this laser action it is necessary to contain photons within the laser medium and maintain the conditions for coherence. This is accomplished by placing or forming mirrors (plane or curved) at either end of the amplifying medium, as illustrated in Figure V.4.

[3] photon with energy hf will not necessarily always stimulate another photon with energy hf. Photons may be stimulated over a small range of energies around hf providing an emission which has a finite frequency or wavelength spread (linewidth).

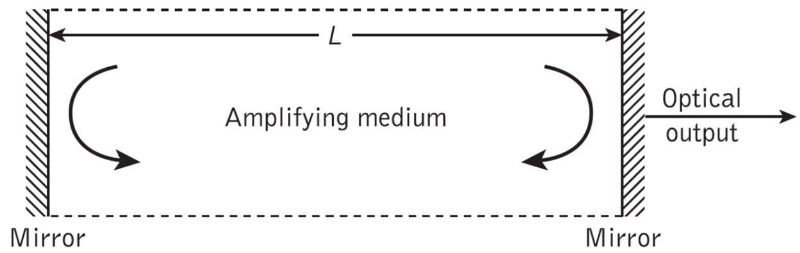

Figure V.4: Basic laser structure with mirrors

The optical cavity formed is more analogous to an oscillator than an amplifier as it provides positive feedback of the photons by reflection at the mirrors at either end of the cavity. Hence the optical signal is fed back many times while receiving amplification as it passes through the medium. The structure therefore acts as a Fabry-Pérot resonator. Although the amplification of the signal from a single pass through the medium is quite small, after multiple passes the net gain can be large. Furthermore, if one mirror is made partially transmitting, useful radiation may escape from the cavity.

A stable output is obtained at saturation when the optical gain is exactly matched by the losses incurred in the amplifying medium. The major losses result from factors such as absorption and scattering in the amplifying medium, absorption, scattering and diffraction at the mirrors and non-useful transmission through the mirrors.

Oscillations occur in the laser cavity over a small range of frequencies where the cavity gain is sufficient to overcome the above losses. Hence the device is not a perfectly monochromatic source but emits over a narrow spectral band. The central frequency of this spectral band is determined by the mean energy-level difference of the stimulated emission transition. Other oscillation frequencies within the spectral band result from frequency variations due to the thermal motion of atoms within the amplifying medium (known as Doppler broadening) and by atomic collisions. Hence the amplification within the laser medium results in a broadened laser transition or gain curve over a finite spectral width, as illustrated in Figure 6.5. The spectral emission from the device therefore lies within the frequency range dictated by this gain curve.

Since the structure forms a resonant cavity, when sufficient population inversion exists in the amplifying medium the radiation builds up and becomes established as standing waves between the mirrors. These standing waves exist only at frequencies for which the distance between the mirrors is an integral number of half wavelengths. Thus when the optical spacing between the mirrors is L, the resonance condition along the axis of the cavity is given by

$$L = \frac{\lambda q}{2n} = \frac{1}{2}\frac{\lambda}{n}q \tag{V.2}$$

where λ is the emission wavelength, n is the refractive index of the amplifying medium and q is an integer. Alternatively, discrete emission frequencies f are defined by:

$$f = \frac{qc}{2nL} \tag{V.3}$$

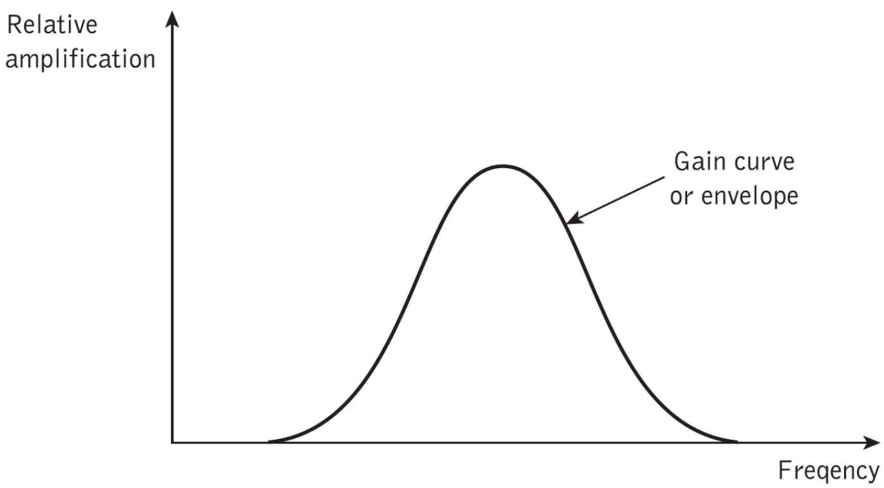

Figure V.5: Relative amplification in the laser amplifying medium

***

VI. Optical Receivers

VI.1. Introduction

Detection of optical signals can be performed using direct techniques or coherent (homodyne or heterodyne) techniques. In the direct detection process of optical signals, the lightwave power is converted by the photodetector (PD) to an electric current. The generated current is proportional to the power in the incident optical field. The direct detection (DD) scheme is illustrated in Figure VI.1.

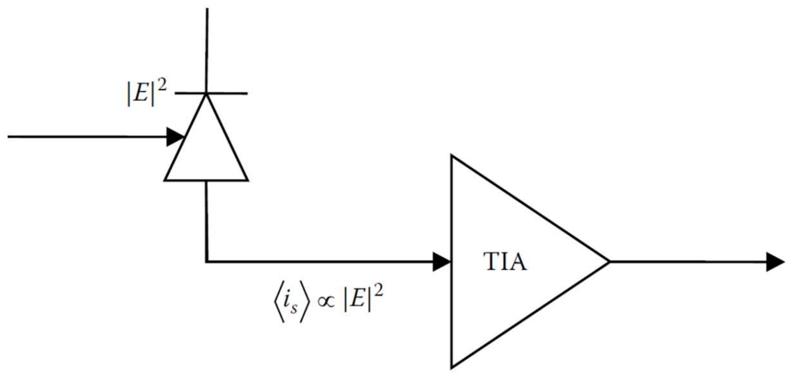

Figure VI.1: Direct optical detection

Using coherent detection, the input optical field is mixed with a local oscillator so that the total field can be detected by the PD. The generated current is proportional to the power in the sum of the incident optical field and the local oscillator field. This square law operation results in components whose frequencies can be either the sum or difference of the signal and the local laser frequencies. The difference term will bring the detected signals back to DC when the carrier frequency of the local laser and the signal carrier is the same, the homodyne coherence detection.

Coherent detection is illustrated in Figure VI.2.

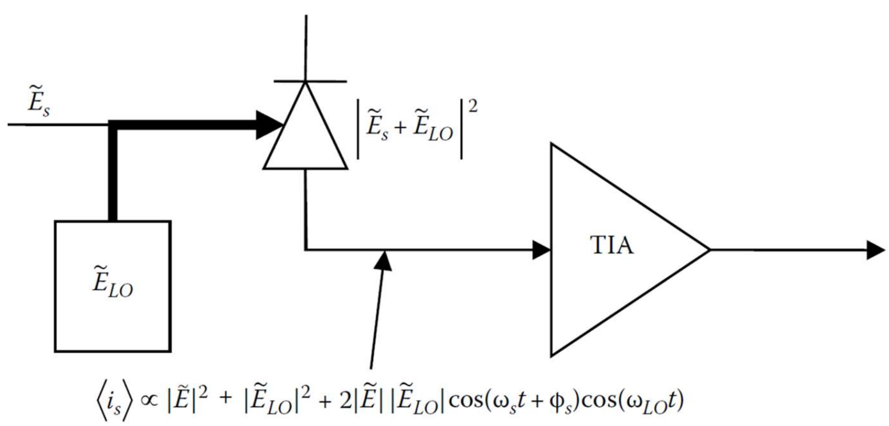

Figure VI.2: Coherent optical detection

This mixing process in coherent detection allows the boosting of the magnitude of the generated current by the magnitude of the local oscillator field.

Optical receivers are normally placed at the far end of the transmission links or they are used in the front end of an optical repeater in terrestrial optical systems and at terminal front ends in optical networks. Their principal function is conversion of optical signals into electronic forms for further electronic amplification and signal processing.

The typical arrangement of an optical receiver is that the optical signals are detected by a photodiode (a pin diode or APD or a photon counting device), electrons generated in the PD are then electronically amplified through a front-end electronic amplifier. The electronic signals are then decoded for the recovery of the original format.

The ultimate goal of the design of optical receiver is to determine the minimum optical energy in terms of the number of photons per bit period required at the input of the PD so that it would satisfy a certain optical signal-to-noise ratio for an analog optical system or the sensitivity of a digital optical communication system satisfying a certain bit error rate (BER). In other words, the minimum optical power is required at a certain bit rate in a digital communication system so that the decision circuitry can be detected with a specified BER, for example, BER = 10^{-9} or 10^{-12}.

VI.2. Receiver Components

The design of an optical receiver depends on the modulation format of the signals that are transmitted by the transmitter. In particular, it is dependent on the modulation being analog or digital, on the used pulse shape, on using on-off keying (OOK) or multiple intensity levels, and so on.

ON/OFF keying (OOK) optical signals are assumed to be generated using intensity modulation (IM). The receiver is assumed to use DD; such that the whole system is referred to as an IM/DD system. It is assumed that light waves arriving at the receiver are polarization-independent and that their polarization plays no part in the degradation of the optical signals. Figure VI.3 shows a schematic of an optical receiver.

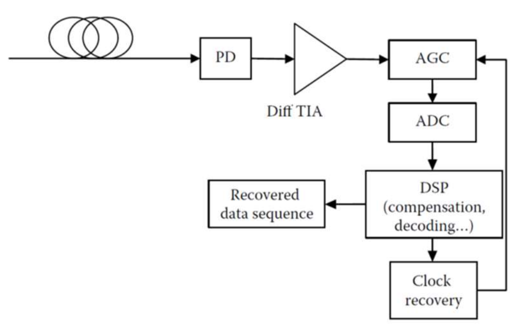

Figure VI.3: Optical receiver

VI.2.A. PHOTODIODES

A PD detects and converts the optical input power into an electric current output. The ideal PD would be highly quantum efficient, would, ideally, add no noises to the received signals, respond uniformly to all signals with different wavelengths around 1300 and 1550 nm, and finally would not be saturated and behave linearly as a function of a signal amplitude.

There are several different types of PDs which are commercially available. In the semiconductor-based types, the photodiode is used almost exclusively for high-speed fiber optic systems due to its compactness and extremely high bandwidth. The two most commonly-used types of photodiodes are the p-type-intrinsic-n-type (PIN) and avalanche photodiode (APD).

PIN Photodiode

As shown in Figure VI.4, a pin PD consists of three regions of semiconductors, the heavily doped p, the intrinsic i, and the n doped sections. It is essential that the pn junction is reverse-biased to cause mobile electrons and holes to move away from the junction, increasing the width of the depletion layer as a result of which a high electric field is produced by the immobile charges at both ends.

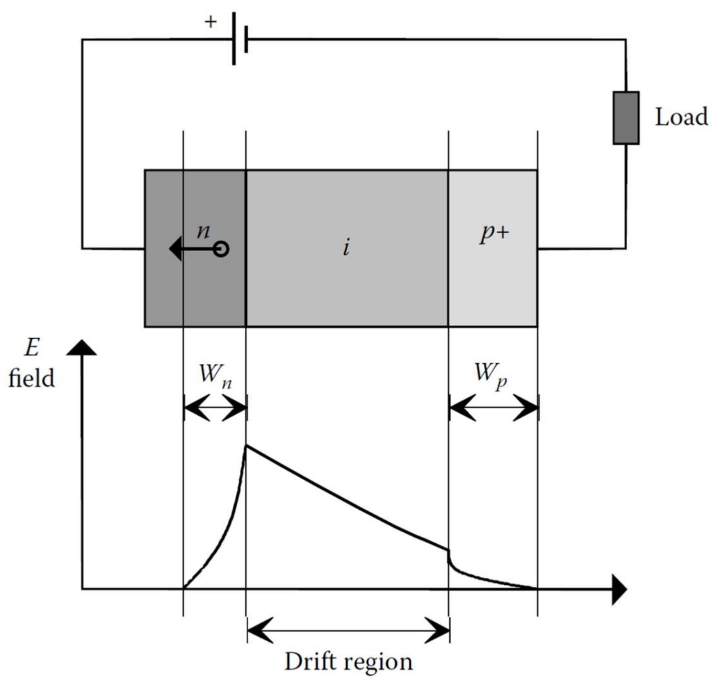

Figure VI.4: PIN PD

If lightwaves are incident on the PIN surface and absorbed in the high-field depleted region, the electron-hole pairs generated will move at saturation-limited velocity. No great contribution is seen if the photons fall in other regions. Thus, since the width of the p region, W_p, is inversely proportional to its doping concentration, decreasing the doping level to intrinsic behavior would widen W_p, and the depleted region will now be wider and compatible with the absorption region to produce large photon- generated current. A p+ region must be added to make good ohmic contact. A wider intrinsic region gives higher quantum efficiency, η but lower response rates.

Avalanche Photodiode (APD)

High-field multiplication region is added adjacent to the lightly doped depletion region (intrinsic) as in contrast with the PIN structure. Photons absorbed in the intrinsic region produce electron-hole pairs. These pairs drift to the high-field region whereby they gain sufficient energy (the E field must be above the threshold for impact ionization to occur) so as to ionize bound electrons in the valence band upon colliding with them. The avalanche effect occurs only when the electric field in the high-field multiplication region is above the threshold for impact ionization (Figure VI.5). A guard ring is usually added to prevent the leakage of surface current, I_{surf}.

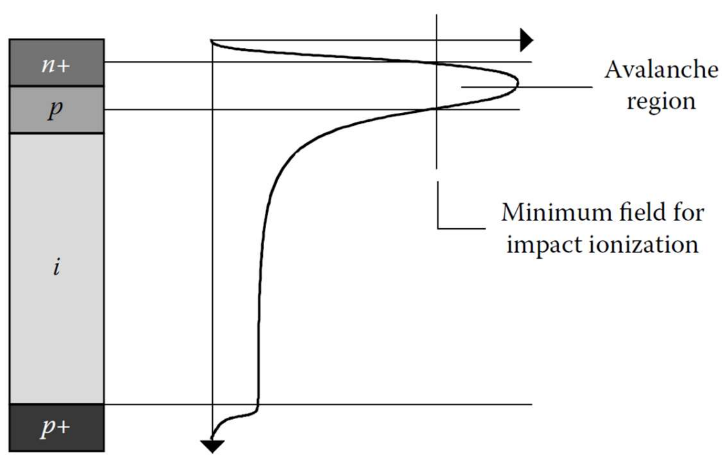

Figure VI.5: APD

Quantum Efficiency and Responsivity

Two most important characteristics of a PD are its quantum efficiency and its response speed. These parameters depend on the material band gap, the operating wavelength, the doping and thickness of the p, i, and n regions of the device. The quantum efficiency η is the number of electron-hole carrier pairs generated per incident photon of energy hf and is given by

$$\eta = \frac{\text{Number of electron pairs generated}}{\text{Number of incident photons}} = \frac{I_p/q}{P_0/hf} = \frac{I_p hf}{P_0 q} \tag{VI.1}$$

where I_p is the photocurrent and P_0 is the incident optical power.

The performance of a photodiode is often characterized by its responsivity $\Re$ which is related to the quantum efficiency by

$$\Re = G\frac{I_p}{P_0} = G\frac{\eta q}{hf} = G\frac{\eta q \lambda}{hc} \tag{VI.2}$$

where G is the APD average multiplication factor. Note that $G = 1$ for non-APD photodiodes.